UNIVERSITY OF CALIFORNIA SAN DIEGO

Locomotion performance of hexapod robots on rough substrates and the influence of leg compliance

A Thesis submitted in partial satisfaction of the
requirements for the degree
Master of Science

in

Engineering Sciences (Mechanical Engineering)

by

Amartya Bhattacharyya

Committee in charge:

Professor Nicholas Gravish, Chair
Professor Mauricio de Oliveira
Professor John Hwang

2019

The Thesis of Amartya Bhattacharyya is approved, and it is acceptable in quality and form for publication on microfilm:

_____

_____

_____
Chair

University of California San Diego

2019

EPIGRAPH

If vitality gives a man's perspective color, if community bonds give them breath, if ***awareness*** *of the land makes them* ***realistic*** *, a deep sense of* ***loyalty*** *gives them personal* ***meaning*** *and integrity.*

—Harry Hunt Ransom

TABLE OF CONTENTS

LIST OF FIGURES

LIST OF TABLES

ACKNOWLEDGEMENTS

I would like to express my immense gratitude to Prof. Nicholas Gravish for his guidance throughout the length of my work in this project and giving me an opportunity to be a part of his lab. I would like to extend my sincere thanks to Prof. John T.Hwang and Prof. Mauricio de Oliveira for attending my defense.

I would also like to thank my parents for giving me the opportunity to pursue my Masters and providing me with both emotional and financial support throughout my stay at University of California San Diego.

To all members of Gravishlab, without the weekly lab updates and your insightful suggestions I don't think this would have been possible.

VITA

2017	B. S. in Mechanical Engineering *5th/120*, NMIMS, INDIA
2018-2019	Graduate Teaching Assistant, University of California San Diego
2019	M.S in Mechanical Engineering, University of California San Diego

ABSTRACT OF THE THESIS

Locomotion performance of hexapod robots on rough substrates and the influence of leg compliance

by

Amartya Bhattacharyya
Master of Science in Engineering Sciences (Mechanical Engineering)

University of California San Diego, 2019

Professor Nicholas Gravish, Chair

Hexapod Robots are a complex system where six legs are connected to the main body which acts as a support frame. A lot of research has been performed in this field from the study of six legged insects to present day implementations where the robot uses its own decision making network. The motivation for this field are the various advantages that hexapedal robots provide like; Obstacle climbing capability, omnidirectional motion, variable geometry, stability, access to uneven terrain etc. At the same time they also have many disadvantages like low energy efficiency, low speeds, complexity of operation and design and especially a lot of attention has to be given to path and gait planning. Therefore, in this paper we

use an open loop platform for our robot and test the performance on simulated rough substrates. Using the results we propose a compliant leg design which will improve the performance while maintaining the stability. We compare the new design with solid legs to quantify the gain. And also test for the shear force limits to make sure the design is ready to be tested on a robot for full length runs. With a goal to utilize the new design and simplify the requirements of complicated neural networks for gait planning.

Chapter 1

Introduction

1.1 Motivation

From the first implementation of Raiberts 3D hopper, over the years legged locomotion has been implemented in various ways. There are bipedal, quadrupedal, Hexapedal and many hybrid robots. Now, wheeled locomotion is power efficient and has a smoother ride due to the constant contact with the ground. But still there is a growing interest in improving legged robots, due to the advantages that they present over wheeled locomotion. Legged robots use discrete footholds for each foot in contrast to wheeled locomotion which needs a continuous support surface. Leading to improved agility on irregular terrain by varying the configurations of the legs to adapt to irregularities. Although, wheeled locomotion is more efficient on hard flat surfaces, legged robots outperform wheeled robots on soft surfaces due to their discrete footholds as they deform the environment less. Also, due to multiple degrees of freedom can change their heading without slippage and can vary their height. Such versatility comes with its own set of limitations. The Higher DOF makes the robot both heavy and difficult to make. Further, the control and gait planning is highly complex. Of all the legged robot designs Hexapedal robots inspired by insects have higher stability in a wider range of velocities.

In our surroundings not many creatures can boast a running speed of almost 50 body lengths per second, to put that into perspective that is a human running at 200 miles per hour, and at the same time climb vertical surfaces and walk

upside-down; these capabilities are strictly limited to insects. This might have been what stimulated the interest of science to study these creatures, with the hope to one day utilize their physical attributes to benefit humans. The initial results of insect studies showed promising possibilities in terms of the static and dynamic capabilities [11][29][27], but also drew attention to the complexity of the anatomy. Cockroaches and Stick Insects were used for most of the studies which revealed the different parts involved in the planning and execution of the locomotion in insects, the legs, thorax and spring like components which acted like muscles [19][28]. The legs constitute of the coxa, trochanters, femur, tibia and tarsus, where each part played a different role and leading to a design with 7DOF. It was observed that insects used repetitive cyclic gaits like alternating tripod, wave, tetrapod etc.,[32][11]for locomotion at different speeds on flat ground and each of these gaits had different dynamics. Of all the gaits it was established that the alternating tripod gait was used by the insects for most of their locomotion as it has high static and dynamic stability for a large range of speeds. The alternating tripod gait is when the front leg and the hind leg of one side and the middle leg of the other side move in tandem. Therefore, there are three legs in contact with the ground at all time. This was only one of the advantages of legged locomotion over wheeled locomotion. In wheeled locomotion we have no control on the vertical ground reaction forces as the movement is purely dependent on rolling friction. In legged design we can control the reaction forces in both the horizontal and the vertical direction and use them to our benefits based on the task defined.

The next logical step was to find ways to implement the concepts into a physical robot. One of the first implementations of the concepts led to a robot with 6 legs and each leg having 2DOF generated by a revolute joint and prismatic joint []. This successfully implemented the tripod gait but also brought up the various challenges to truly replicate insect locomotion. The robot was limited to linear motion and had no capability to tackle any obstacle. Following this a lot of concepts were developed like Compliance, Gait Generation, Elevator Reflex, Searching Reflex, Turning and Integration of Reflexes [9]. This lead to the creation of Robot

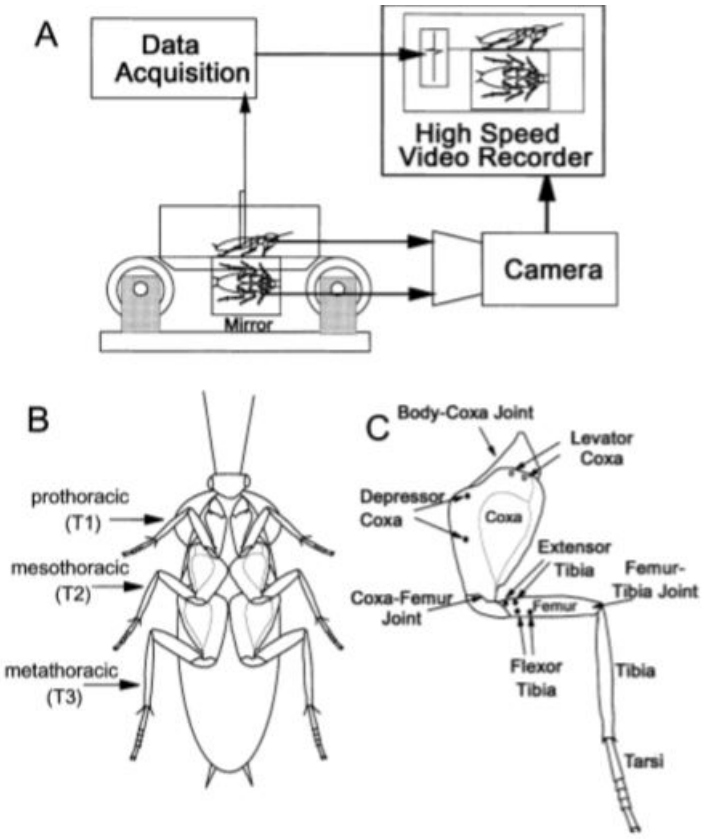

Figure 1.1: (A) The experimental set-up for simultaneous electromyography and high-speed videography. (B) Blaberus discoidalis. (C) Leg of B. discoidalis, showing recording sites for recordings from depressor coxa, levator coxa, extensor tibia, and exor tibia. The dark circles indicate recording site on the ventral surface, and the open circles indicate recording sites on the dorsal surface of the leg. [28]

(R1), Laron, TUM and many more hex pedal robots which were focused on improving maneuverability [21]. The years following saw iterative versions of the robots mentioned above trying to perfect the design through their own innovative approaches. Now, robots in simulation were as good as insects to avoid obstacles but were exceeding slow and heavy and were slowly being limited by the available technology for any significant advancement.

This prompted research in a new direction to achieve higher velocities with lower power consumption. This was achieved using various techniques like under actuation and designs with only 6 DOF in comparison to 18DOF or even 42DOF.

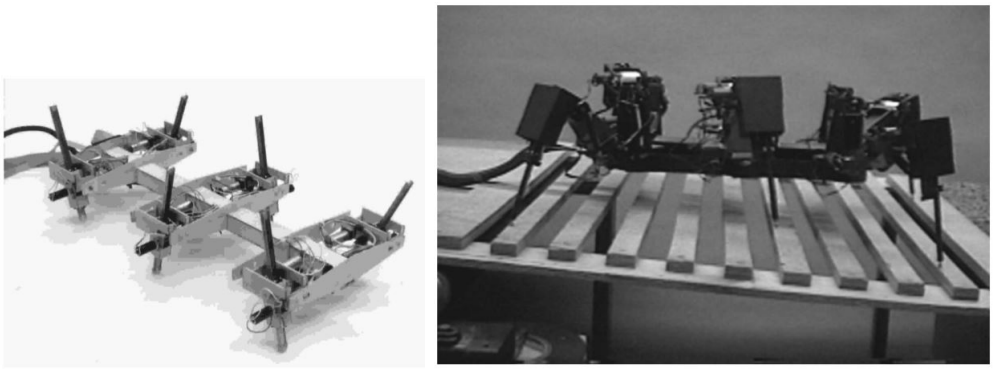

Figure 1.2: Robot 1 (left) with 2DOF. Robot 2(right) with 18DOF. [9]

This led to the creation of RHex, Whegs, DynaRoach, DASH, Sprawl and many more [24] [2] [17] [25] [14] [18].

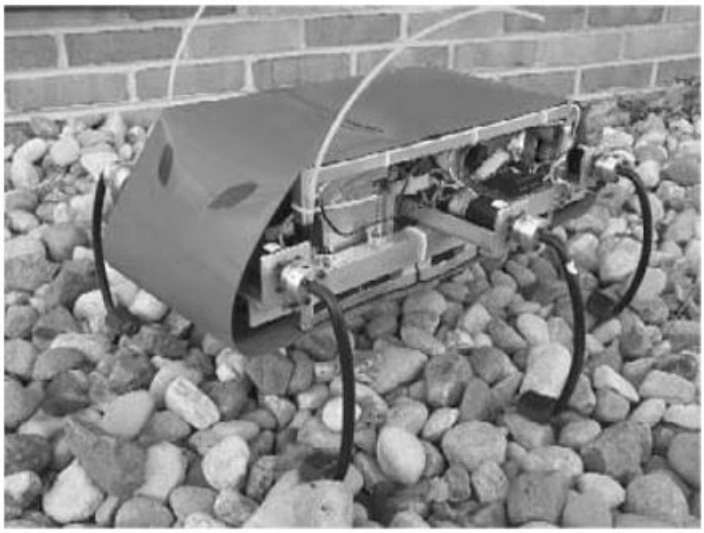

Figure 1.3: RHex experimental platform. [24]

Over the years many attempts have been made to implement the concept of Distributed Mechanics and biologically inspired neural control along with detailed analysis of the application of the various gaits. [16] [9] Through which it was repeatedly proven to achieve omnidirectional locomotion only 3DOF per leg was enough.

In this work we used an open loop control hexapod with 18DOF, 3DOF per leg which we will refer to as the hip, thigh and foot. The goal of the project was to understand the impact of a compliant leg design on the performance of our robot using tripod gait on varying substrates. The substrates chosen were flat (to set a performance parameter) and simulated rough surfaces. The rough surfaces were simulated using a checkerboard pattern of different sizes (3inches and 5inches) with every other block having a height of 1inch. This design was chosen as we wanted to establish a correlation between the no. of interactions with an obstacle in a run and the performance of the robot. The performance was gauged by the phase of the hip joints and the path traced by the robot in a run. We observed a possible relation between the height of the obstacle and the distance from the obstacle in relation to the stride length of the robot. A retrofit compliant leg was designed to maintain similar kinematics and control. Following which a new test rig was designed to focus on the interactions and compare the success between the rigid and compliant leg designs.

Chapter 2 Introduces the different parts of the Robotic Setup. It first glances over the concept of geared servos and the type of servo that we chose. Then it talks about the robot as a whole, covering the design considerations and fabrication techniques. It also covers the concept of inverse kinematics and how it was implemented for the design finalized for out experiments. Lastly, it introduces the concept of the Beetag which is used to track the motion of the robot during the experiments.

Chapter 3 Focuses on the Tripod Gait Analysis by first introducing the cameras and the math behind the calibration and the inverse transform which is a crucial aspect of the experimentation in our trials. It then moves on to the Different substrates designed and used to simulate a rough substrate with regularly intervaled obstacles. Once the hardware is defined we cover the code execution of the robots and the pattern in which the data-flow was setup. We then immediately delve into the experiments and present the ideas in chronological order with the servo data analysis first followed by the Tracking data analysis. The chapter ends with

a small summary of the analysis and the results to prepare the reader for the next chapter which covers the design of the new leg.

In chapter 4 using the results and conclusions of the previous chapters we define the reasoning behind the choices for the design of the new compliant leg. We then discuss the experimentation performed along with the setup and results. We conclude the chapter with a summary of the results to build the idea of the possibilities of future work.

In the last chapter we discuss the possibilities of future development and the different avenues to explore to further improve performance with distributed mechanics.

1.2 Current State of Art

Under-actuated designs with low degrees of freedom are ideal to achieve high velocities for locomotion, some instances of such Designs are like Rhex. [24] A hexapod robot with each leg being actuated by a single motor. It tests the performance of the robot on varying terrains studying its speed and orientation. The motivation of this robot was to overcome the lack of control over the vertical force generated by the ground reaction forces in wheels. The leg was designed as a single spoke of a wheel and by controlling the angle at which it contacted the ground, were successfully able to control the reaction forces both in the horizontal and vertical direction. The robot was primarily open loop therefore an external visual analysis system was implemented. The robot utilizes an alternating tripod gait to move, with a 180 degree phase difference between the left and right tripods. This design was the inspiration to WHEGS. Which as the name suggests an acronym for legs inspired by wheels (WHeels and LEGs). This was an iterative approach to build a series of robots following WHEGS called WHEG2 and mini-Whegs. Whegs2 added a hinge in the main body of the robot to assist with vertical climbing and mini-whegs as the name suggests was a miniature design of the original to achieve higher speeds. Two more well known robots with a similar concept were developed called DASH and Dynaroach [14] [2].Both were geared towards a miniature design

to truly replicate the kinematics of a cockroach.

Figure 1.4: Whegs2 (left) the hinge in the middle was added to assist with climbing. MiniWhegs(right) next to a blaberus gigantius for scale.[25]

Another series of robots that is worth mentioning is the Sprawl series[17]. Especially Sprawlita improved the performance of a hexapod robot by changing the power-train. The older designs were pneumatically actuated using a piston. Which limited the scale of the robot as beyond a certain size it is almost impractical to carry an, on board gas tank with the required power. The new design implemented a flexible cable with low friction. The advantages of the new design over the old one was realized using the ground reaction forces in both cases, and analyzing the change in the trajectory of the hip joint due to the passive compliant leg design.

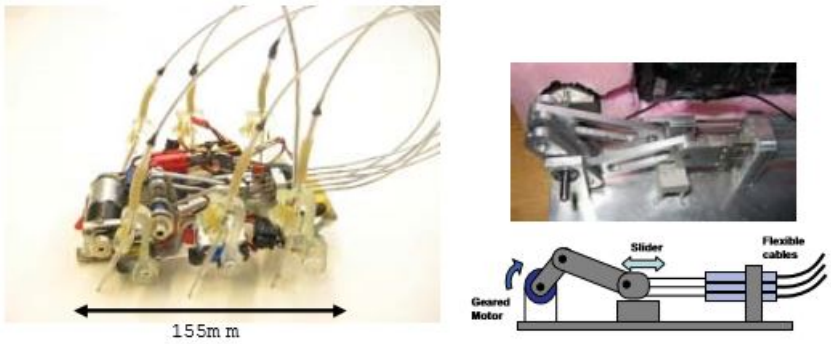

Figure 1.5: Isprawl(left) using flexible cable design. The mechanism of the flexible cables(right).[17]

Now focusing on the designs which focused on improving the maneuverabil-

ity of the robot using the distributed mechanics mentioned in [9]. The different mechanisms were compliance, stepping reflex, elevator reflexes, searching reflexes, turning, gait generation, Integration of reflexes. Compliance is the use of passive elasticity in the leg improving the performance of the robot on rough terrains. Stepping reflex is the corrective mechanism to recover from a significant perturbation compromising the stability of the robot. Elevator reflex is the control mechanism if the leg is blocked by an obstacle then it doesn't end its swing and looks for a surface at a higher angle. Searching reflex is the counter to the elevator reflex when a robot is stepping down form a higher surface it will keep looking for a stable foothold. These are modelled on the probing nature of insects. Turning in robots can be achieved in different ways depending on the design of the robot. Some require a different gait with ipsilateral synchrony in contrast to contralateral while some designs can use a tripod gait to turn.

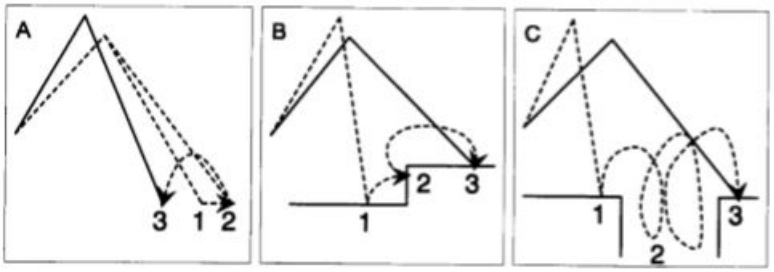

Figure 1.6: A Stepping reflex. B Elevator Reflex. C Searching Reflex[9]

The paper [30] models a gait for a hexapod with only one actuator and compliant legs to execute both linear motion and turning by modulating the orientation of the body and stiffness of the springs. The legs are assumed to be mass-less and therefore the force acting at the tip of the foot is assumed to be the force acting at the hip joint. Another paper uses SMA(shape memory alloys) to design a 18DOF hexapod, where the alloys work as a compliant leg design [5].

[15]This paper attempts to model a robot with a R-Slip rather than SLIP. Where a circular leg design is modified with the addition of a torsional spring.

The design constitutes a circular leg with a bar connected to one end of the leg with a torsion spring and the other end to the robot for the input of motion. The new model was tested on a robot like the R-Hex robot which is based on the SLIP model and uses the linear elasticity of the leg design. The control of the robot was completely open loop with initial programming of the trajectory planning. The observed advantage was that the new R-Slip design provided a larger angle for stable point contact with the ground. Also, the stable range of the angle increased with the increase of the speed.

Focusing on the past 10 years, along with new designs to achieve better performing robots many papers have performed independent analysis of the tripod gait implemented in their designs.

One such paper develops an inverse kinematic implementation of the tripod gait to improve static turning by changing the design to permit a larger sweep angle with smaller overlapping. Then tests the proposed method on a real hexapod with success under the assumed conditions that the contact between a foot and the ground is a point, there is no slipping between the foot and the ground, and all the mass of the legs is lumped into the body and the center of gravity is assumed to be at the center of the body [6].

Another paper studied the influence of each leg during free walking experiments on plane surfaces with incline ranging from 0Deg to 90Deg [12]. It reinforces the importance of the front legs in locomotion of insects, which includes synchronous patters with adjacent legs and multiple stepping asynchronous to the adjacent legs for probing. However, the coordination of the middle legs and the hind legs are crucial for walking. In one of the tests performed middle leg amputees were used were there was no consistency between contralateral and ipsilateral synchrony between the front and hind legs. [13] This paper inspects a robot with 18DOF both numerically and experimentally through dynamic modelling using tripod gait on flat and hard grounds. The ground reaction forces, and energy consumed by the

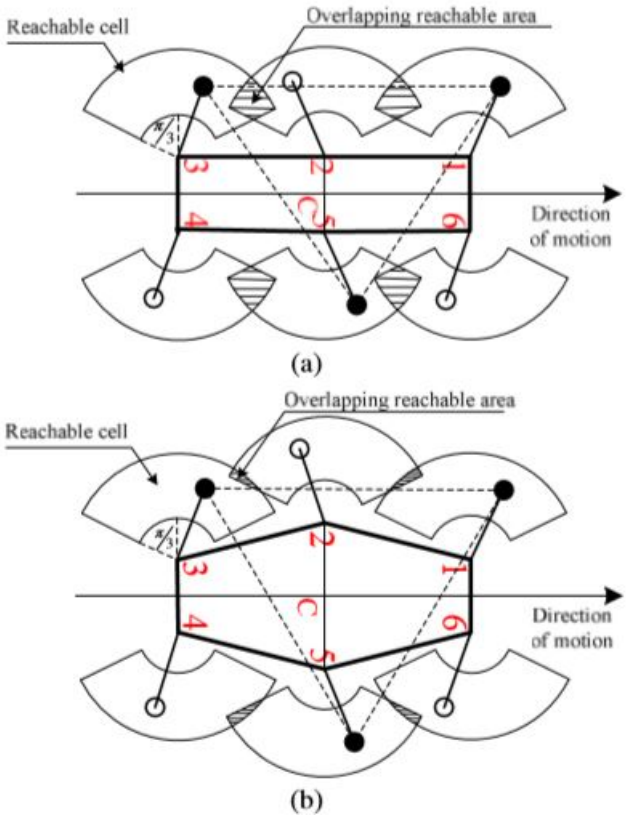

Figure 1.7: a) The reachable area in a simple rectangular design. (b) The reachable area in the proposed design.[6]

robot in gaits generated by 4 different Central Pattern Generators are analyzed. The goal was to find an energy efficient model for long running use of Hexapods. [31] This paper proposed a CPG based locomotion control to get the obstacle dimensions and decide to either surmount the obstacle or avoid it.

There are not many papers that have focused on the passive nature of the legs and the effect of preflexes on the Robot when it encounters obstacles. One paper does such an analysis of the legs of cockroaches. [7]This paper studies the recovery time in response to a perturbation in cockroach legs. The idea was to find the difference in the behavior of the legs when the joints are fixed and not fixed. At low speeds the cockroach behaved like a stick insect where it has a neural approach to overcome obstacles. But, at higher speeds the effect of the perturbations were not as pronounced leading to the hypothesis that the legs had some passive damping

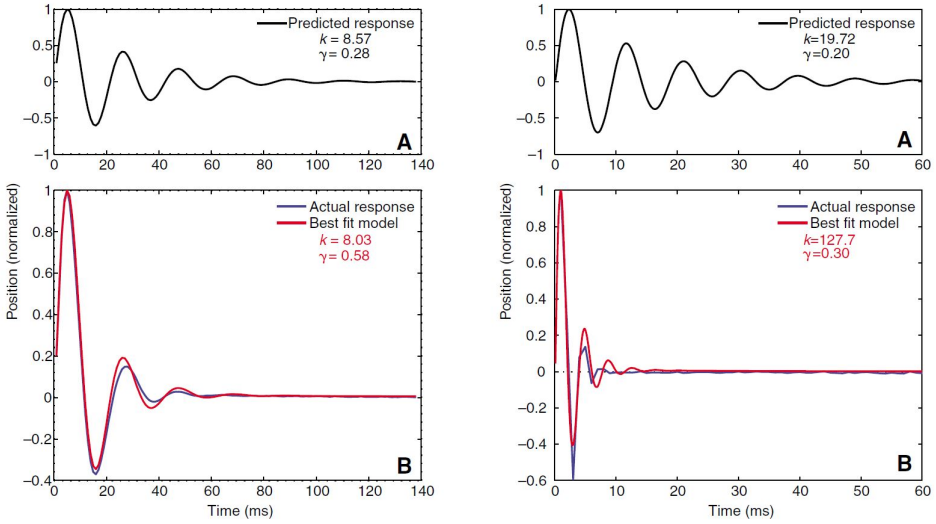

Figure 1.8: Response of the metathoracic leg with a freely rotating bodycoxa joint to an impulsive perturbation(Left). Response of the metathoracic leg with a fixed bodycoxa joint to an impulsive perturbation(Right).

capacity. To test this, the legs were amputated from cockroaches and then tested with a rigid coxa, and rigid coxa and femur joints. It was observed that when the joints were free the ability of the leg to absorb the perturbation was more but as it was a part of the movement of the leg during the swing and stance phase the time for recovery almost 20ms. In the cases where the joints were fixed the stiffness of the legs were more, but the recovery from the perturbation was in approx. 5ms. About $1/4^{th}$ the duration of the first case. This supported the claim where the cockroaches at higher speeds do not neutrally control the flexibility of the legs but depend of distributed mechanics and can hence maintain high speeds even on rough grounds.

Chapter 2

Robotic Setup

The design of the robot is crucial to the goals of any experiment. There are many aspects to consider in terms of the physicality of the robot like the Leg Types, Leg Orientation, and Leg Configuration. In this paper the goal was to analyze the performance of the Hexapod on rough substrates. The motivation of the paper is to mimic the dynamics of an ant and achieve improved performance in an open loop environment with compliant leg designs [32]. We needed a design which had a high static and dynamic stability and the capability to recover from slight perturbation [27]. Along with the aforementioned requirements we also wanted omnidirectional movement in the robot [6].

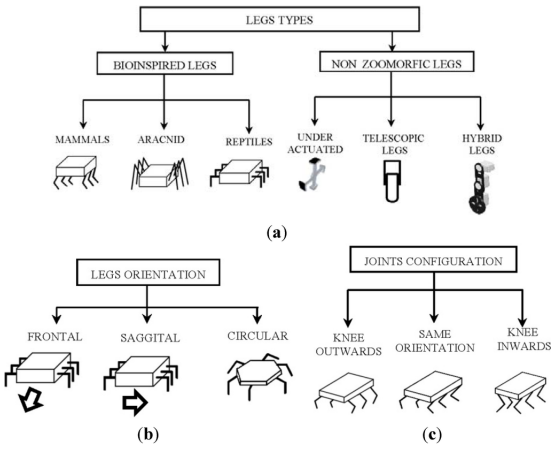

Figure 2.1: The different possible hexapod configurations.[26]

Therefore, we finalized on a Circular design with outward knees to get a sprawled position. The robot has 18 DOF total with 3DOF in each leg divided into the Hip, Thigh and Foot.

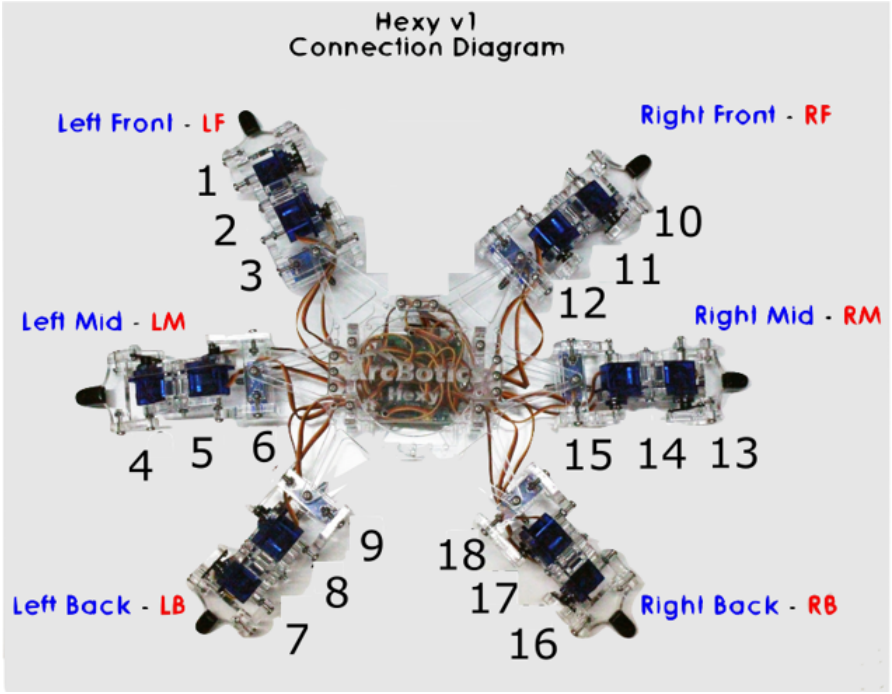

Figure 2.2: The finalized design with the wiring to each of the servos

2.1 Servos

2.1.1 Introduction to Servos

A servo motor is a rotary actuator that consists of a motor coupled to a sensor for position feedback. It requires a servo drive to complete the system as it uses the feedback sensor to precisely control the rotary position of the motor.

The problem with controlling a standard RC servo motor from a microcontroller is that it is 'closed loop' inside the servo motor case, but 'open loop' with respect

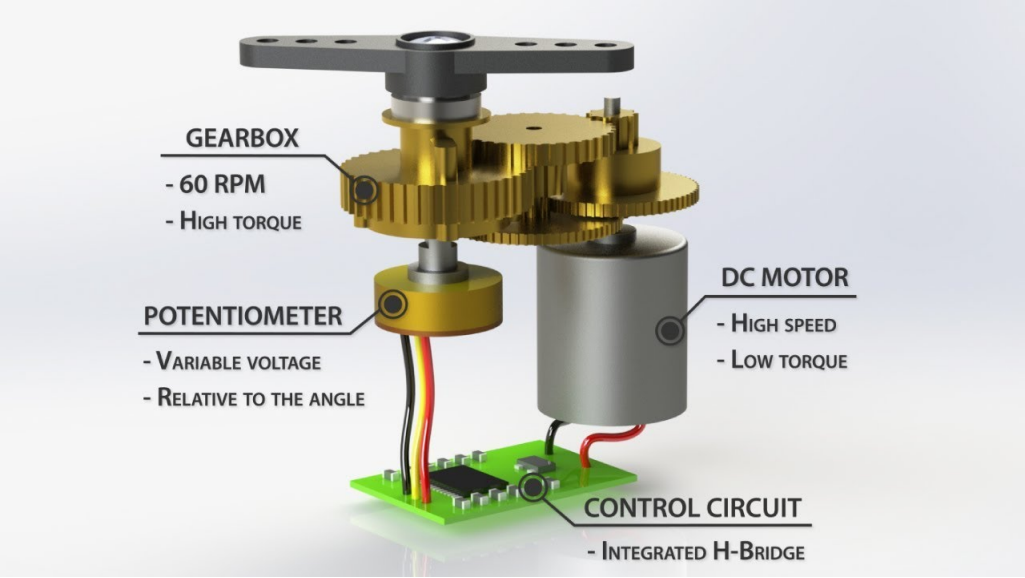

Figure 2.3: Parts of a Servo Motor

to your microcontroller. You can tell the servo control circuit how you want the shaft positioned, but you have no way to confirm if or when this happens.

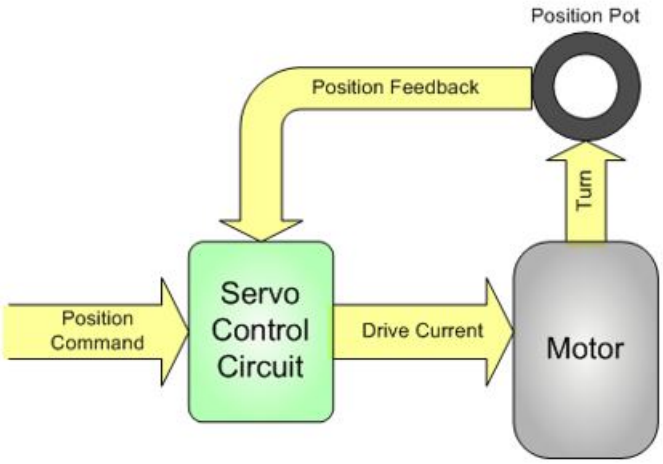

Figure 2.4: Internal Closed loop of a Servo Motor

2.1.2 Servo Used in Robot

One of the parameters that the paper uses as a performance measure during a run, is the true position of the hip joint which represents the phase of the whole leg. To get a reading of the true position of the servo we used a servo motor which had a connection from the inbuilt potentiometer available which gave us access to the analog feedback of the voltage. We mapped the specifications of the motor in terms of the voltage range and the maximum angle to get the true position of the joint.

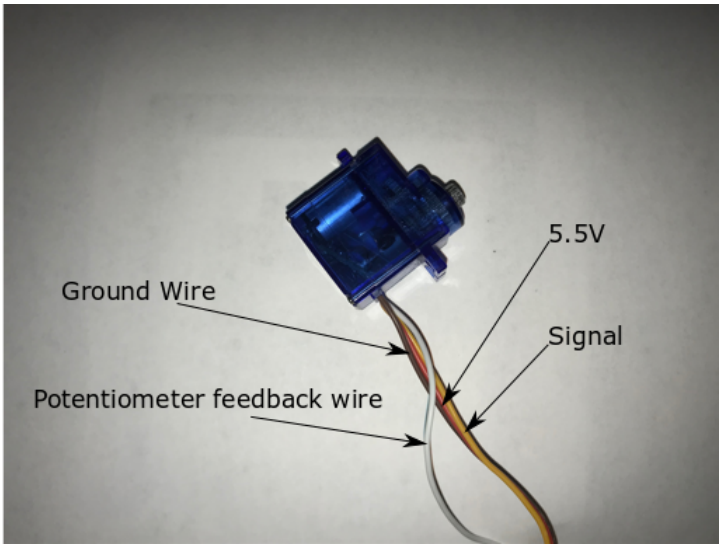

Figure 2.5: Metal gear servo with analog feedback of voltage

2.2 Microcontroller

A microcontroller is a compact integrated circuit designed to govern a specific operation in an embedded system. A typical microcontroller includes a processor, memory and input/output (I/O) peripherals on a single chip. Usually microcontrollers have pins which act as connectors and can be programmed to different signal types. There are three different signal types Analog, Digital and PWM.

Table 2.1: Specifications of Servo Motor used in this paper

Material	Aircraft-grade aluminum gearing
Feedback	Analog Voltage position feedback
Size	21x12x22 mm
Voltage	3V - 6V
Weight	14g
Speed	0.12 sec/60(4.8V)
Torque	2.5kg-cm
Working Temp	-30C - 60C
Brushing	Aluminum
Wire	25cm wire
Motor	core-less motor

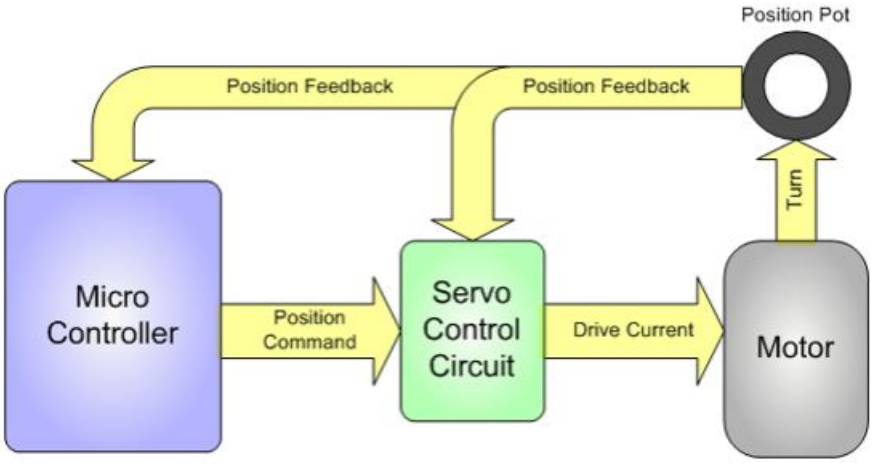

Figure 2.6: Semi closed loop feedback of position

2.2.1 Types of Signals

Analog Signals

An analog signal has a continuously varying value, with infinite resolution in both time and magnitude. A nine-volt battery is an example of an analog device, in that its output voltage is not precisely 9V, changes over time, and can take any real-numbered value. Analog voltages and currents can be used to control things directly, like the volume of a car radio. In the servo motor the potentiometer turns along with the shaft of the motor. As it turns the resistance goes up or down

leading to the current also changing.

Digital Signals

Digital signals are distinguishable from Analog signals because digital signals only take values only from a finite set of predetermined possibilities, such as the set 0V, 5V. In practical application that is significant to the on and off a switch.

PWM Signals

PWM is a way of digitally encoding analog signal levels. Using high-resolution counters, the duty cycle of a square wave is modulated to encode a specific analog signal level. The PWM signal is still digital because, at any given instant of time, the full DC supply is either fully on or fully off. The voltage or current source is supplied to the analog load by means of a repeating series of on and off pulses. The on-time is the time during which the DC supply is applied to the load, and the off-time is the period during which that supply is switched off. Given an enough bandwidth, any analog value can be encoded with PWM. One of the advantages of PWM is that the signal remains digital all the way from the processor to the controlled system; no digital-to-analog conversion is necessary. Increased noise immunity is yet another benefit of choosing PWM over analog control, and is the principal reason PWM is sometimes used for communication. Switching from an analog signal to PWM can increase the length of a communications channel dramatically.

2.2.2 Signal Input/Output Pins

Digital Pins

Digital pins can be either inputs or outputs and can either read or write digital signals (0 or 5V).

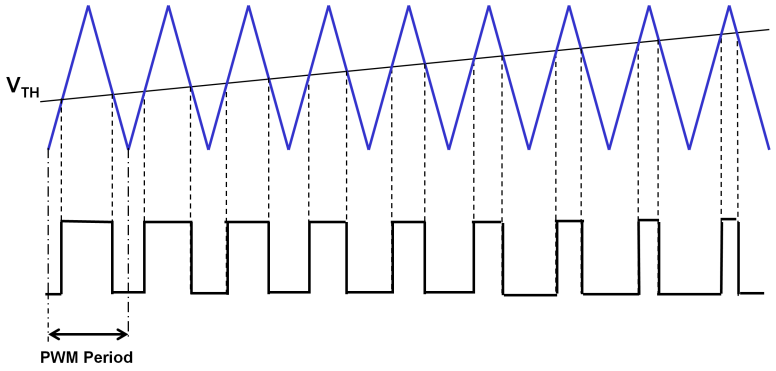

Figure 2.7: Converting an Analog signal to PWM

Analog Pins

Analog Pins can read analog voltages between 0V and 5V. Most microcontrollers have an analog-to-digital converter circuit that reads this voltage and converts it to a single 10-bit value (a number between 0 and 1023). Where 0 represents 0V, and 1024 represents 5 V.

PWM Pins

Some digital pins can also output pulse-width-modulation (PWM) signals, which are square signals with different duty cycle. This is a way to produce a similar effect of an analog voltage. Digital pins produce either a high or low digital voltage level but many external circuit components require analog voltages. PWM produces an output whose net effect is similar to an analog voltage in the range of 0-5V but varies the duration of the high and low voltage levels.

2.2.3 Servotor32

The hexapod has 18DOF, therefore we needed a board with at least 18 servo pins. We used a Servotor 32 which as the name suggests has 32 servo pins and is Arduino compatible.

Table 2.2: Servotor32 Specifications

Processor	Atmega32u4 @16mhz
Servo Pins	32
Analog Pins	8
PWM	4channels
Digital Pins	14
Other	Ultrasonic Distance Sensing module plug, Slot or Bluetooth-Serial Converter

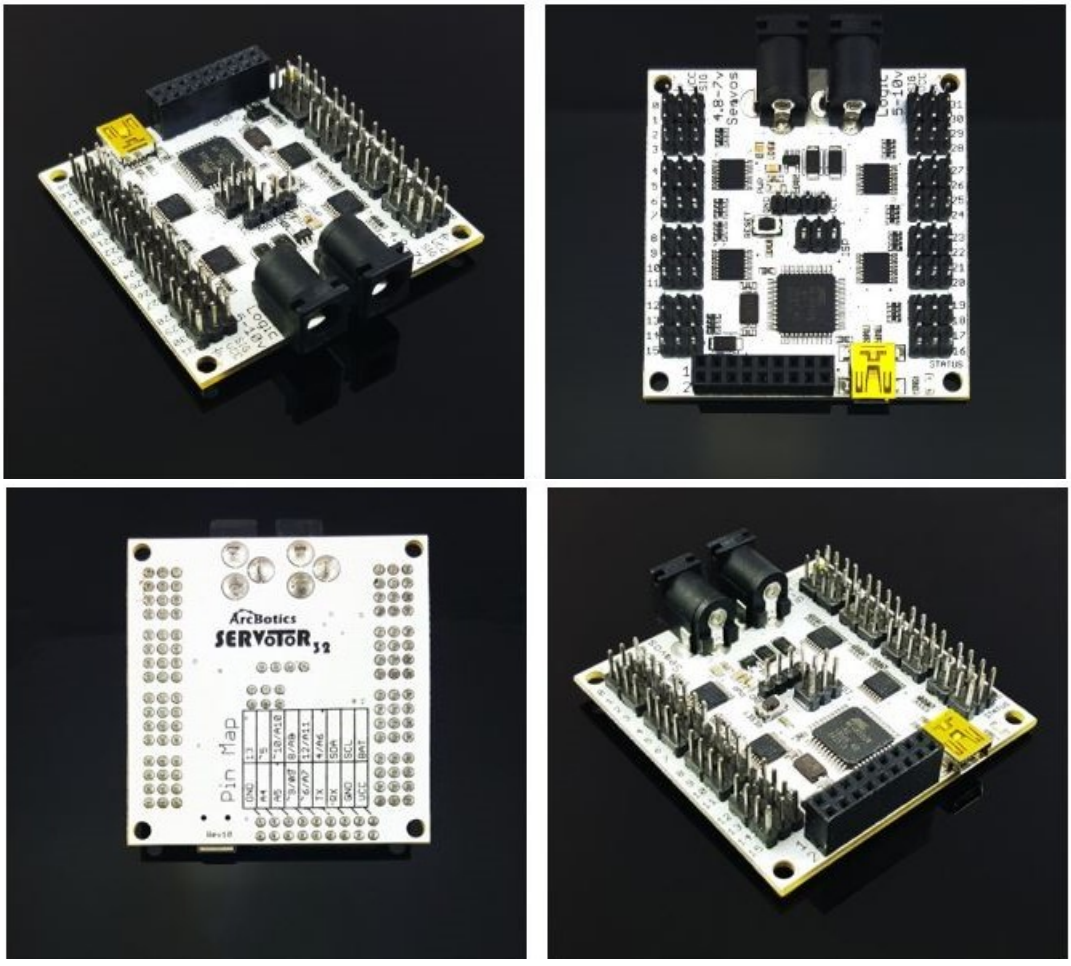

Figure 2.8: Servotor32

2.3 Robot

2.3.1 Material

As discussed above the design finally chosen was circular with a sprawled position for better stability. The weight of each servo is 14g adding to that the weight

Figure 2.9: Glowforge used to laser cut the parts of the robot

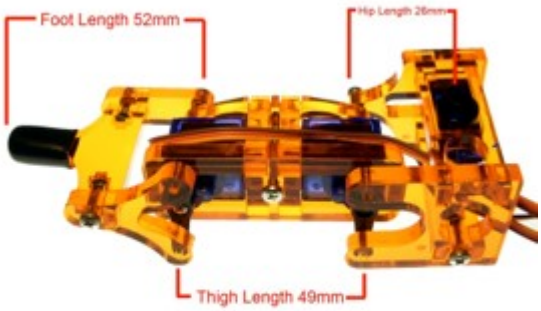

Figure 2.10: The dimensions of the different parts of the leg

of the board and wires would all contribute to the final weight of the robot. It was crucial to maintain the weight of the robot as light as possible to have a higher power to weight ratio. Since in the case that one leg got stuck then the entire load is put on that leg which can be detrimental to the life of the robot. Therefore, we chose quarter inch acrylic as the main material for the robot. The fabrication of the robot was done using a glow forge laser cutter for higher precision.

2.3.2 Kinematics

For the robot to have minimum slip on contact it was crucial for the foot to meet the ground perpendicularly. Therefore, using inverse kinematics different orientations were tested. For simplicity of computation, we assumed instance where the limbs are static. With the legs being a combination of 3 Revolute joints where the Hip rotates in a plane parallel to the ground and both the thigh and the foot rotating about the same axis. We considered only the joints of the thigh and the

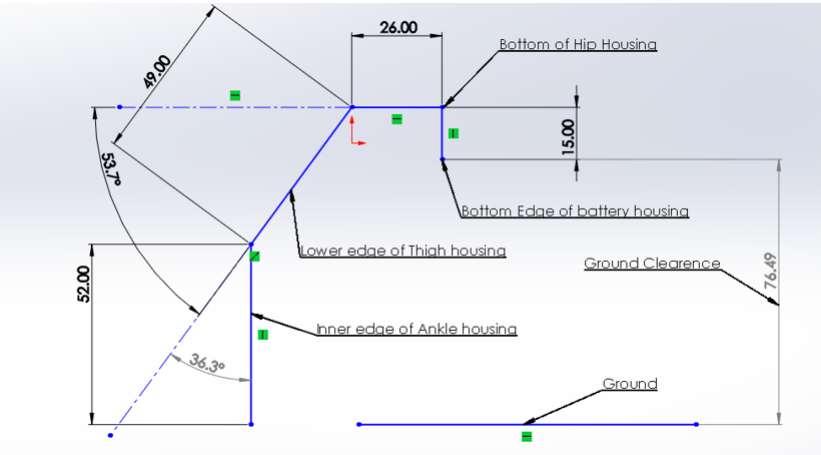

Figure 2.11: Specifications of the leg design

foot leading to a 2x2 matrix . To speed up the process we used an inbuilt tool called RoboAnalyzer to test multiple orientations simultaneously.

Forward Kinematics

This analysis is performed to get the position of the hip joint in reference to a ground reference (world coordinates). Where we use the DenavitHartenberg parameters (also called DH parameters), which include the joint variables and the length of each section of the leg. The limbs of the robot form a 3DOF serial manipulator with three revolute joints. Now using the D-H parameters which are: link length (a_i), link twist (α_i), joint distance (d_i) and joint angle (θ_i), we can form the homogeneous transformation matrix between frames.

Table 2.3: D-H parameters for legs[23]

Joint	θ_i	α_i	a_i	d_i
Coxa	$q_{i,1}$	90	d_i	0
Femur	$q_{i,2}$	0	d_2	0
Tibia	$q_{i,3}$	0	d_3	0

The homogeneous transformation matrix that describes the translation and rotation between frames i and $i-1$ [20], is shown in Eq.:

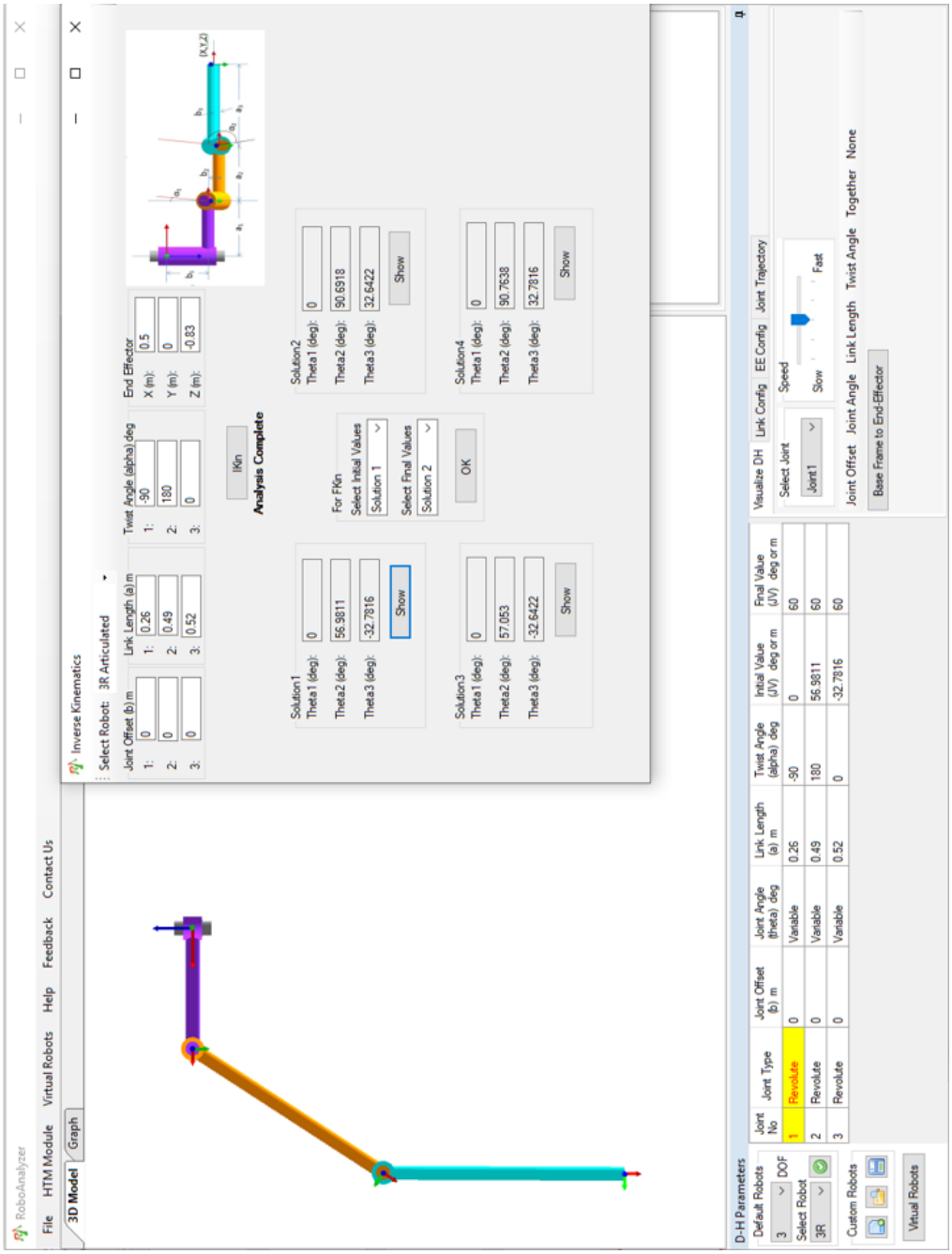

Figure 2.12: Inverse Kinematics using the algebraic method

$$T_i^{i-1} = \begin{bmatrix} cos\theta_i & -sin\theta_i cos\alpha_i & sin\theta_i sin\alpha_i & a_i cos\theta_i \\ sin\theta_i & cos\theta_i cos\alpha_i & -cos\theta_i sin\alpha_i & a_i sin\theta_i \\ 0 & sin\alpha_i & cos\alpha_i & d_i \\ 0 & 0 & 0 & 1 \end{bmatrix} \tag{2.1}$$

Using the above equation we can sequentially calculate the transformation matrix

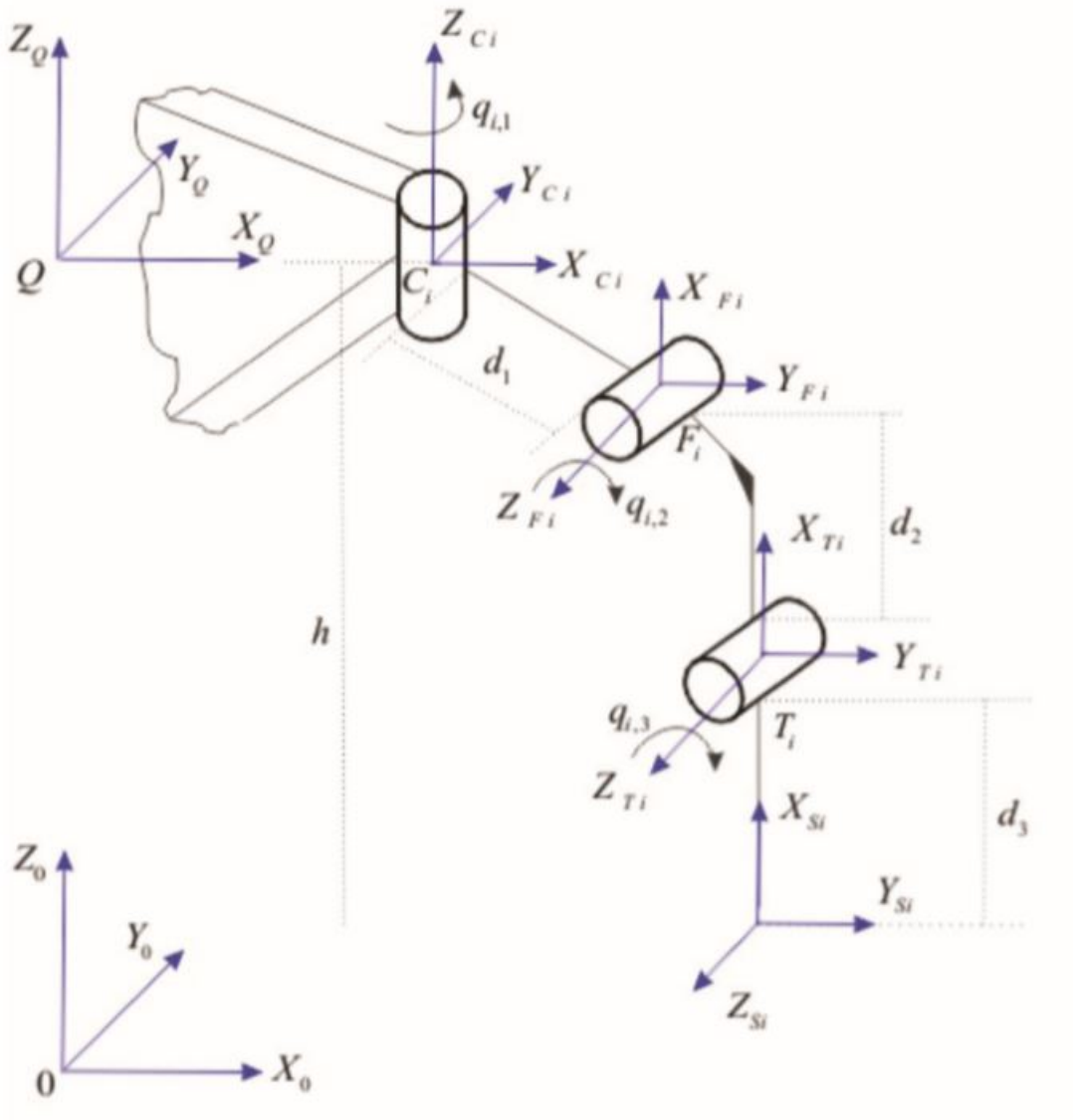

Figure 2.13: Diagram representing the three joints with their orientation and relation to the ground reference [23]

for each joint in respect to the next.Where c represents the Coxa, F represents the

Femur, T represents the Tibia and S represents the foot:

$$T_{S_i}^{C_i} = T_{F_i}^{C_i} T_{T_i}^{F_i} T_{S_i}^{T_i} \tag{2.2}$$

$$T_C^S = \begin{bmatrix} n_c x & o_c x & a_c x & p_c x \\ n_c y & o_c y & a_c y & p_c y \\ c_c z & o_c z & a_c z & p_c z \\ 0 & 0 & 0 & 1 \end{bmatrix} \tag{2.3}$$

2.3.3 Inverse Kinematics

This analysis is performed to get the required angles of the joints based on the desired position of the end effector. It is solved for each leg independently with the considerations that 1. all joints permit rotaion about one axis, 2. the thigh and foot rotate about parallel axes, 3. The physical limit of each leg defining the range of motion. The postion of the end effector is defined in reference to the ground reference.

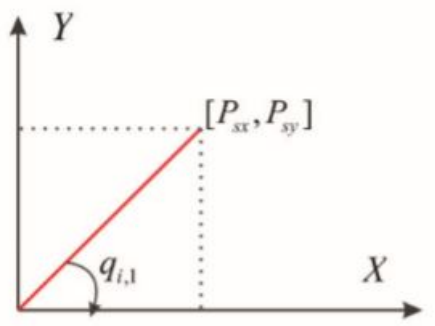

Figure 2.14: Projection of the i-th leg onto the ground representing the position of the end effector in reference to the ground reference [23]

$$q_{i,1} = tan^{-1}(c, \pm\sqrt{a^2 + b^2 + c^2}) - tan^{-1}(a, b). \tag{2.4}$$

where,

$$a = 2d_2(\sqrt{P_{scx}^2 + P_{scy}^2} - d_1), \tag{2.5}$$

$$b = 2P_{scz}d_2, \tag{2.6}$$

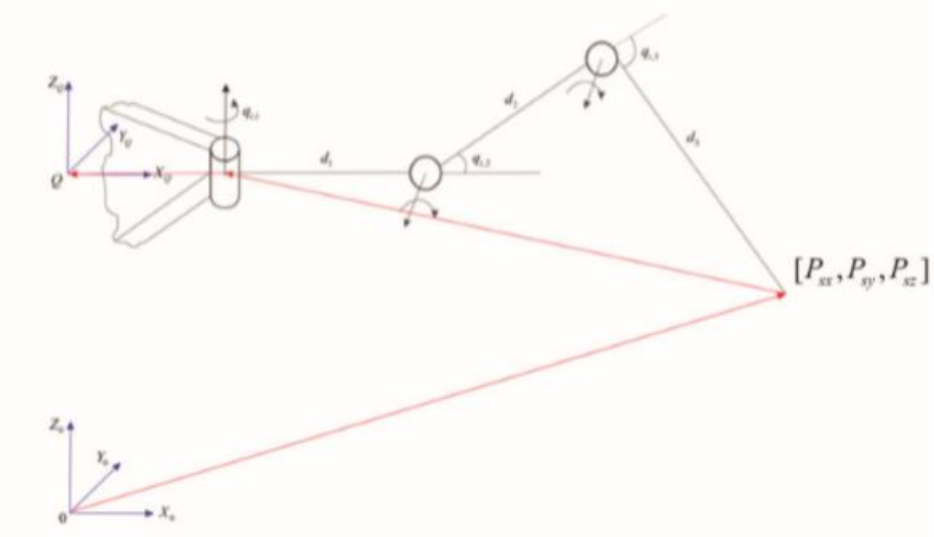

Figure 2.15: Configuration of i leg

$$c = (\sqrt{P_{scx}^2 + P_{scy}^2} - d_1)^2 + P_{scz}^2 + d_2^2 - d_3^2, \tag{2.7}$$

$$q_{i,3} = cos^{-1}[\frac{(\sqrt{P_{scx}^2 + P_{scy}^2} - d_1)^2 + P_{scz}^2 - d_2^2 - d_3^2}{2d_2d_2}] \tag{2.8}$$

2.4 Feedback Micro-controller

Since position of the servos was one of the performance parameters, we needed to record the analog output values from the servos. The microcontroller was already at full capacity with the input to the servos. Therefore, we needed to use a secondary microcontroller which could accommodate 18 analog pins and be light enough to not affect the dynamics of the robot significantly. We chose TEENSY 3.5 as our secondary microcontroller as it satisfied all the above conditions and is compatible with the Arduino IDE.

We mounted Teensy on a breadboard with heads soldered on. Then connected 18 servos to it and one wire from the microcontroller to maintain the same ground. This setup was housed atop the already existing setup. This was done to maintain the autonomy of the robot. As a separator we used cardboard to maintain the weight as low as possible.

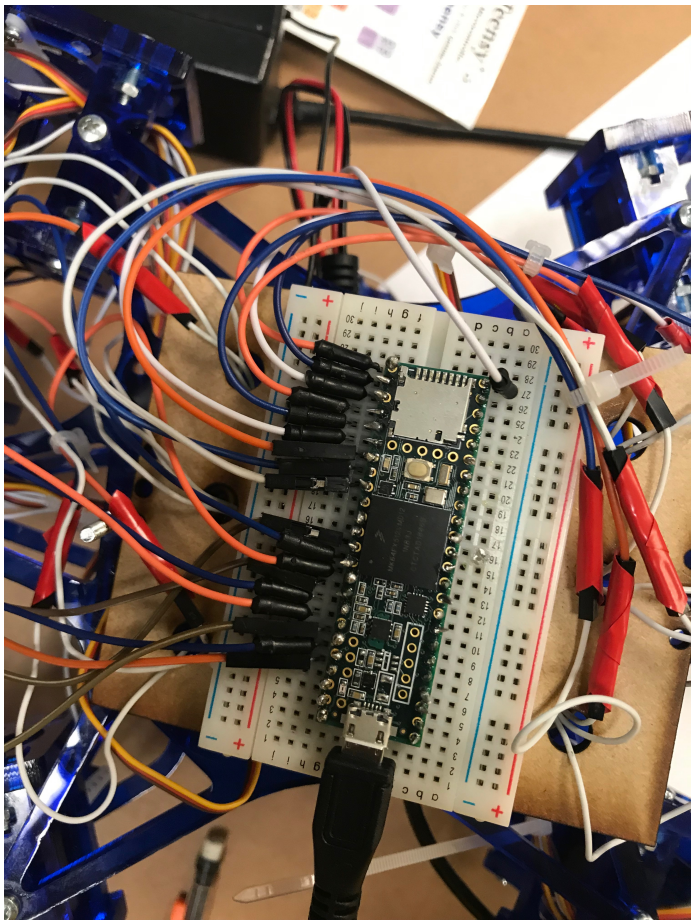

Figure 2.16: TEENSY3.5 to record the analog output from the potentiometer

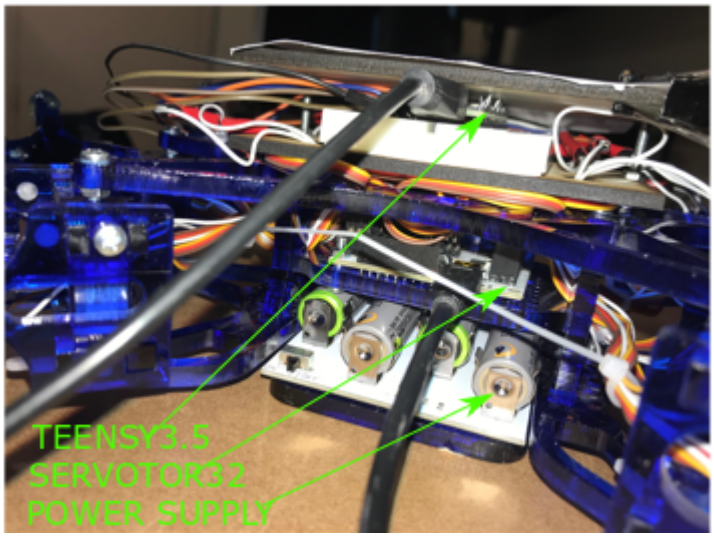

Figure 2.17: Modifications made to house TEENSY on board the robot

2.5 Tracking

The potentiometer gave us information regarding the individual interactions of each leg with the rough surface. But to get a higher level analysis of the entire robot we felt it essential to track the path traced by the robot. To understand how the robot responded to obstacles and if it was able to self-stabilize and continue movement in a straight line. To trace the robot we needed an external tracking setup. We chose BEETAG [3] since it is reliable at varying distances and cheaper to setup

2.5.1 BEETAG Concept

BEETAG was inspired by similar tag designs such as ARtag(Fiala, 2005) and CALTag(Atcheson, Heide, & Heidrich, 2010). The tag consists of a 25bit(5x5) code matrix that is unique to each tag. It is represented by black and white pixels and each code is enveloped in one white pixel border within a 2balck pixel border. It consists of a 15bit identity code and a 10bit error check. The identity code is a 5x3 matrix which represents a number from 1 to 32767 left padded with zeros. In the error code the first three bits are parity checks for the three columns of the 5x3 matrix. The next two bits check the parity of the first 3 and last 2 columns. This is then repeated and reversed to form the 10bit error check. Now this tag can be scaled to any size with the only requirement being it be visible to the camera clearly.

2.5.2 Identifying BEETAG across frames

Each tag is uniquely identified across every fame of the video. The frame is converted from color to greyscale and then threshold into black and white image. The thresholding step converts the matrix of continuous pixel intensity values of an image into a binary matrix using a specific threshold value. This leads to a binary image with zeros as black and ones as white and then checks to see which of them are rectangular and marks them all as possible tags. The software then reads the pixel values within each white rectangle and converts the values from black and

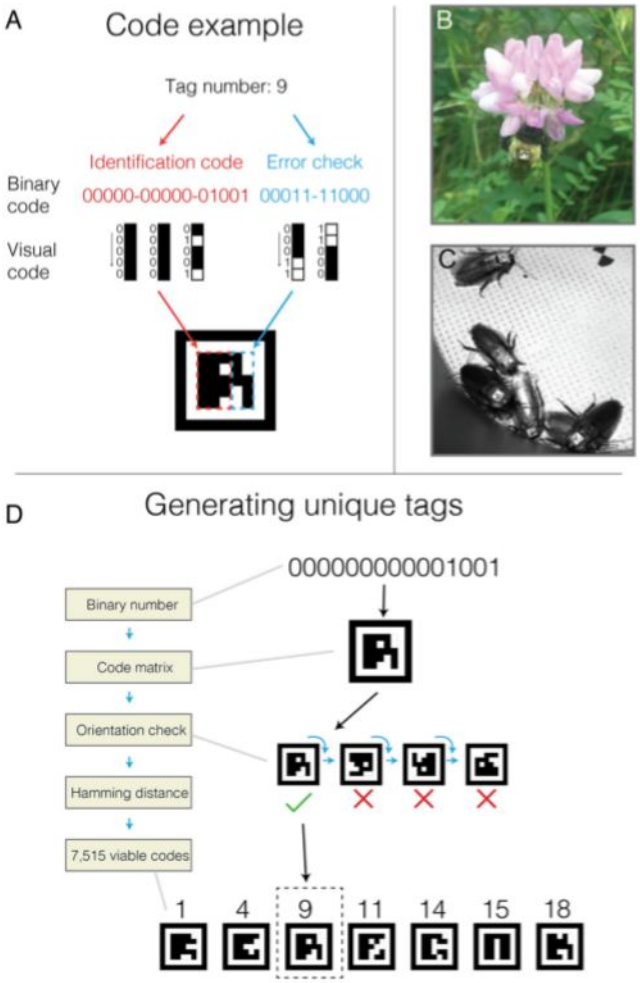

Figure 2.18: BEEtag code structure and generation.(A) Basic tag design.(B) A bumblebee worker (Bombus impatiens) outfitted with a BEEtag and encountered opportunistically in the natural environment.(C) Cockroaches (Blaberus discoidalis) outfitted with BEEtags.(D) Schematic representation of the process for generating a list of unique,usable BEEtags.[3]

white to binary and references them to the list of viable tags. The identity position and orientation of each of the tags are then recorded and stored in an array in the Matlab Workspace.

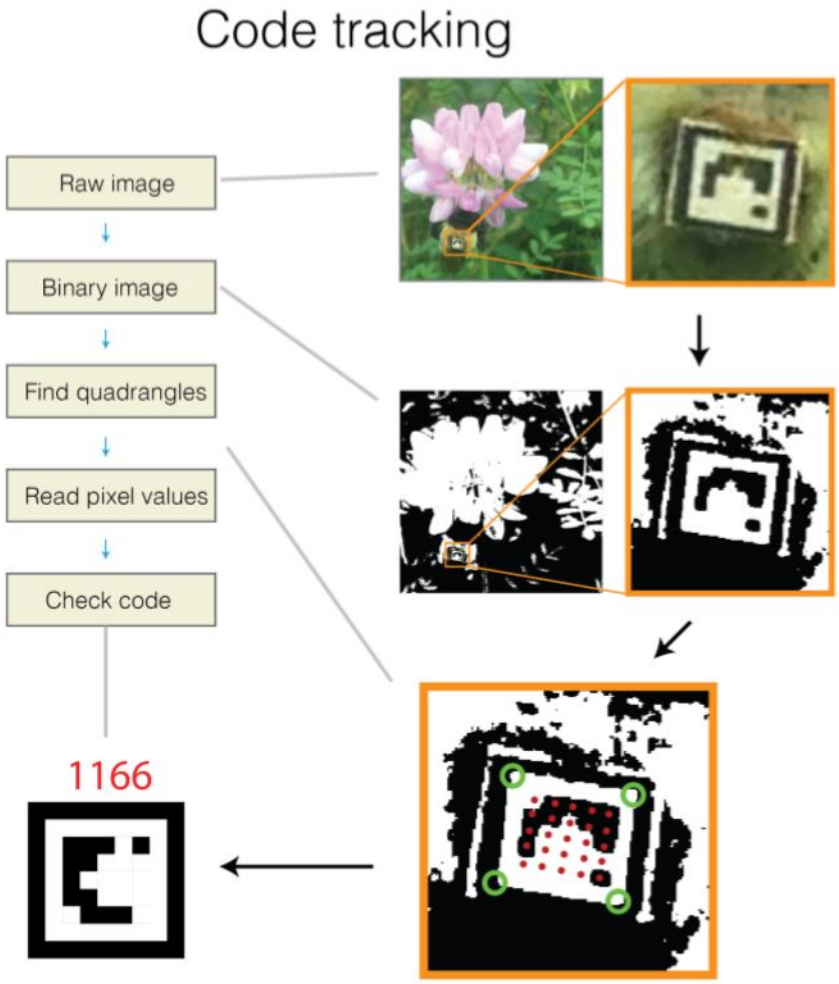

Figure 2.19: Schematic representation of the algorithm for identifying unique BEE-tags from an image. Green circles show identified corners of the white quadrangle, and red dots show points where separate pixel values were measured.[3]

2.5.3 BEETAG no.14

We used a Tag dimensions 6x6inch as the distance of the robot form the camera setup was 1.3m. The bigger tag was necessary since the robot would oscillate slightly on every step which led to the tag not being recognized in every frame.

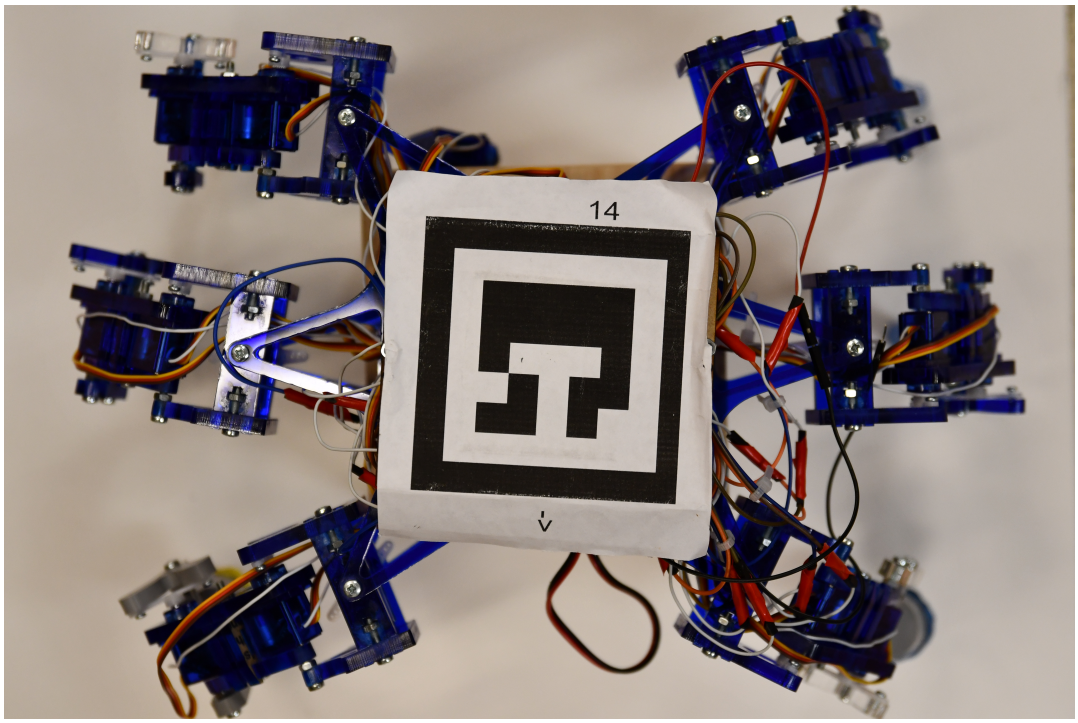

Figure 2.20: BEETAG housed atop the robot

The beetag needed to trace the true center of the robot therefore needed to be housed on top of the already modified housing for TEENSY. Another layer of cardboard was added on which the tag was placed. The orientation of the tag was not essential to the data collected since the path traced was not dependent on it. The data points stored from the software were the centroid location in each frame and the corners of the bounding square in each frame.

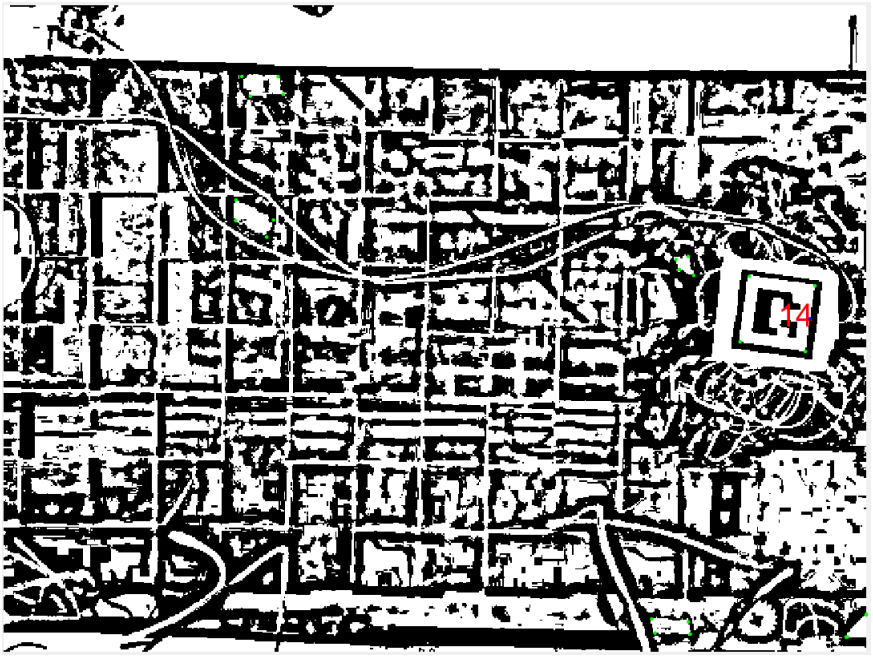

Figure 2.21: Output of Tracking Code

Chapter 3

Tripod Gait Analysis

3.1 Substrates

3.1.1 Design

The first part of the project was to test the performance of the robot on a rough surface. Our initial hypothesis proposed the possible relation between the performance across a run and the frequency of interactions the robot undertakes. To test this idea, we designed lab-based physical simulations of rough surfaces to have control over the no. of possible interactions the robot could face in a run. One of the parameters that we chose to base our design on was the practical clearance of the robot. We chose a checkered pattern of alternating raised blocks. Where the height of the raised block was set to 25.4mm which is approximately 2/3rd the practical clearance of the robot. During a forward swing the thigh joint is coded to go to 0Deg and simultaneously the foot is coded to go to 90Deg to maintain the perpendicularity of the foot when contacting the ground. This was a future proofing the robot incase it faced a higher obstacle to always make perpendicular contact with the ground. Therefore, even though based on the design of the robot the available ground clearance is 76.49mm due to the code the practical clearance is 39.49mm. The other parameter that we chose was the stride length of the robot(44mm). To avoid the instance of the robot stepping over the obstacle we chose dimensions greater than the stride length. The two substrates we finalized

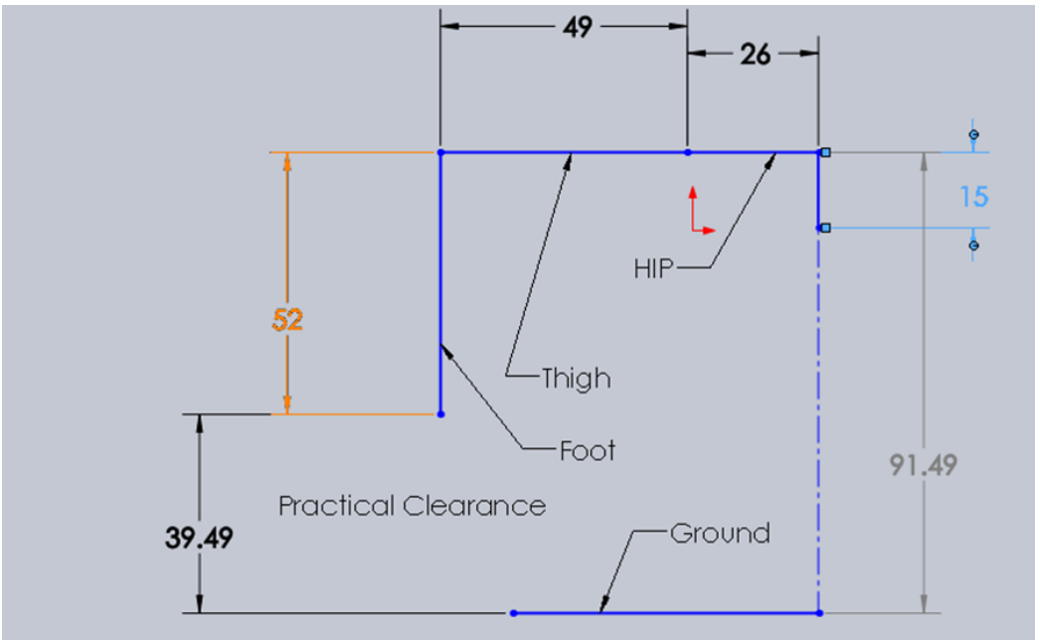

Figure 3.1: The practical clearance available due to the requirement of the foot maintaing perpendicularity with the gorund.

on were squares of 76.2mm(3inches) and 127mm(5inches).

3.1.2 Material and Fabrication

When choosing the materials for the substrates the main conditions were coefficient of friction to prevent slipping and ease of fabrication. Maintaining the above conditions, we chose Acrylic as our material for the substrates. This allowed us to try out different designs and sizes. We used a laserCamm to cut the 0.5inch Acrylic into the required shapes. Then used adhesives to hold the pieces in place. We used a 4x2feet board of acrylic as the base on which the cut pieces were placed. To maintain the consistency of the material in contact with the feet.

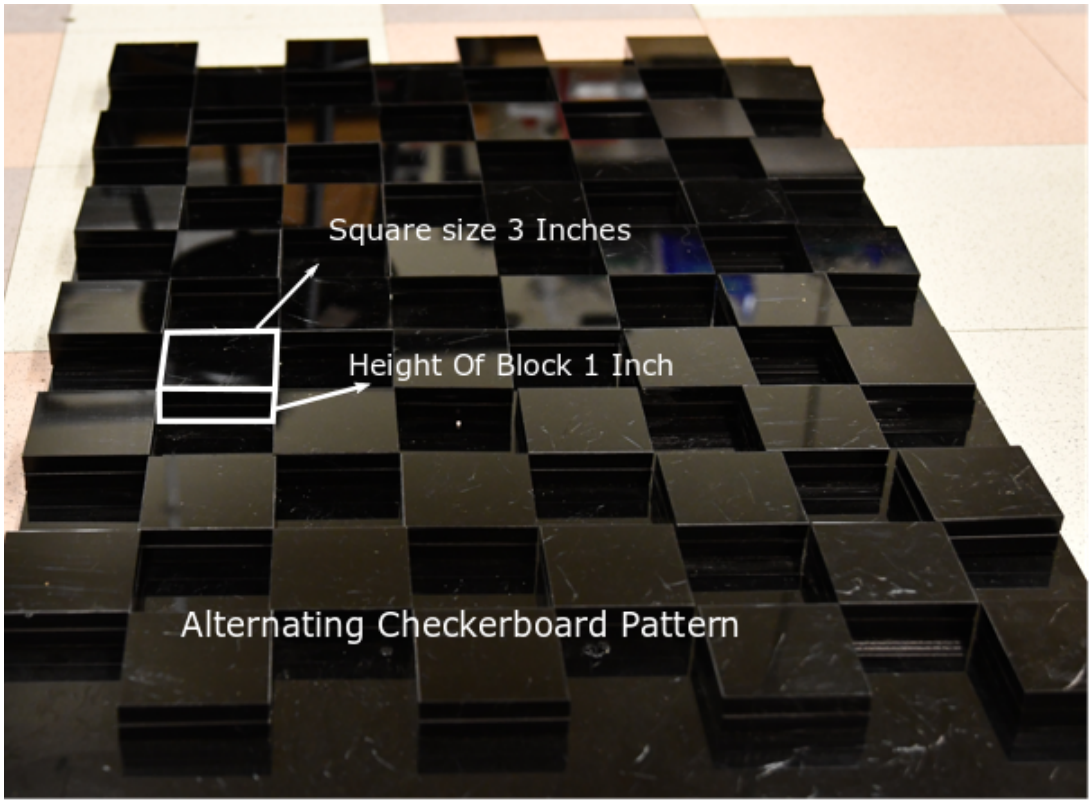

Figure 3.2: Top view of the 3inch substrate

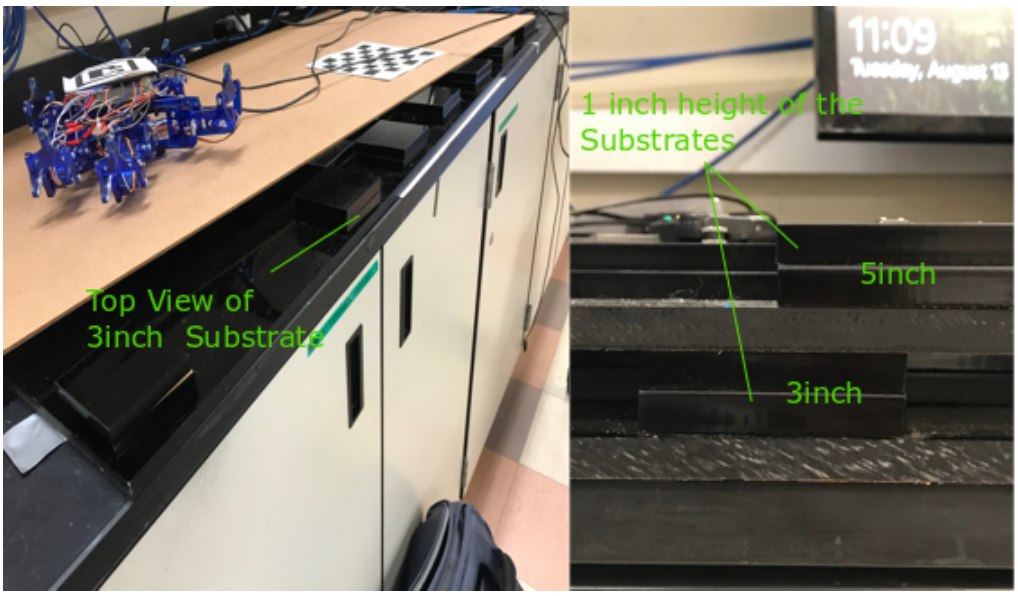

Figure 3.3: 3inch Substrate(left), Height of obstacles(right)

Figure 3.4: LaserCamm used to fabricate the substrates

3.2 Tracking Setup

3.2.1 Camera Selection

The tracking code looks for probable matrices in every frame to get a positive id of the tag and then records the position of the centroid based on the pixel value. There were two ways in which the frame could be dropped by the camera either the robot moves to fast for the camera to get a clear frame or the camera autofocusses away from the robot. The first issue was an effect of out effect of our experiments, so could no be prevented. The second issue can be avoided by manually controlling the focus. Also, the camera had to be light and have a strong hinge as the setup needed to be permanent. Since any disturbance would affect the calibration.

3.2.2 Orientation

The first challenge was to choose between a single or multiple camera setup. The advantages of a Single camera setup are that the computation of data is less. Post-processing is also easier as we would be working with a plane rather than 3D

Table 3.1: Camera Specifications

Lens& Sensor Type	Plastic,CMOS
Focus Type	Fixed
Field Of View (FOV)	60Deg
Focal Length	4.4mm
Optical resolution	1280x960
video Capture(16:9 W)	640x480
Frame Rate(max)	30fps @ 640x480

Figure 3.5: Overhead Camera Orientation

space. The disadvantages were possible error in data without a factor to check the accuracy of the tracking. By only tracking in a plane some important features of the motion may be lost due to perspective. Therefore, we chose to have a dual camera setup. The next step was to decide the position of the setup in reference to the robot and the possible path that the robot was to traverse. The first option was to place it at an angle of 40Deg incline to the center of the board. This would help us understand the yaw and pitch of the robot better. Due to the nature of the lens and the source of light this was ineffective. Since parts of the track were not within scope and towards the edge there was some warping too. Therefore, we chose a higher position (approx. 80Deg) to record the runs. The final position of the camera was at 1.45m from the track vertically and 0.2 m from the center of the track horizontally.

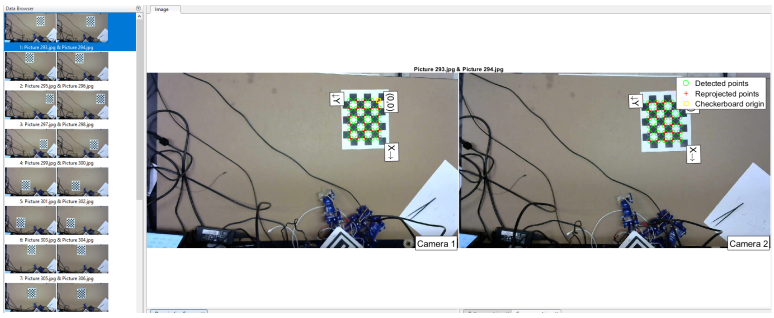

Figure 3.6: Images of checkerboard pattern at different positions to calibrate the camera

3.2.3 Calibration

To recover the 3d position of the robot in reference to a ground reference it was crucial to calibrate the cameras correctly and then maintain the same orientation. We used the stereo calibration app in MATLAB to calibrate the cameras. Which uses one of the stereo pair as a reference point.

Forward Transform helps predict where in an image the world coordinates will appear. It is also called the camera model, which takes the form of a $4x3$ matrix and converts 3D world coordinates into 2D image coordinates. There are many ways to derive a camera model, we are presenting a method which is easy to state mathematically. Assuming the image plane coordinates to be U and V; in homogeneous coordinates an image point is (u,v,t).

$$U = \frac{u}{t} \tag{3.1}$$

$$V = \frac{v}{t} \tag{3.2}$$

If the Camera model matrix is C, with elements C_{ij}. Then for any world point (x, y, z) a C is needed such that

$$(x, y, z, 1)C = (u, v, t) \tag{3.3}$$

$$u = (x, y, z, 1)C_1 \tag{3.4}$$

$$v = (x, y, z, 1)C_2 \tag{3.5}$$

$$t = (x, y, z, 1)C_3 \tag{3.6}$$

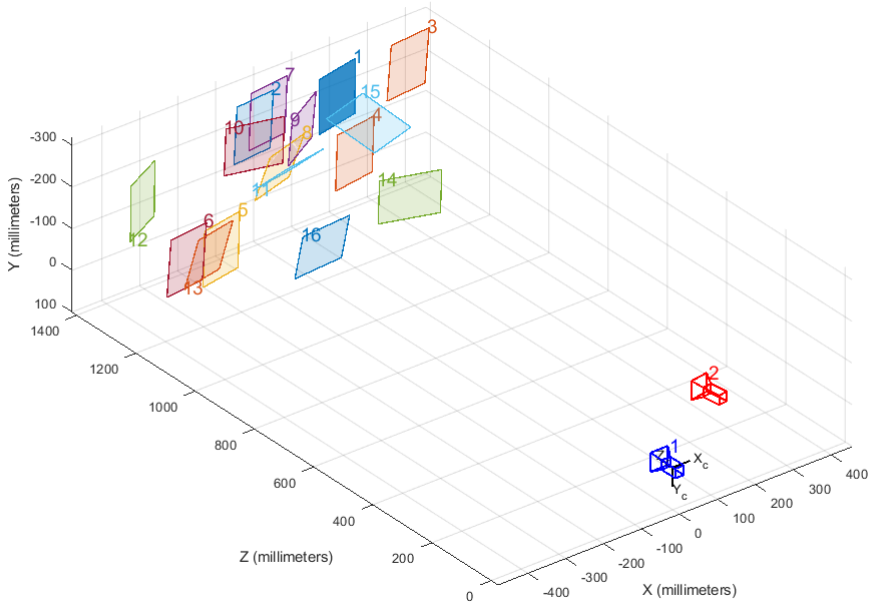

Figure 3.7: Camera-centric representation of the different positions of the calibration object after common frame referencing

Expanding the inner products and rewriting $u - Ut = 0$ and $v - Vt = 0$

$$xC_{11} + yC_{21} + zC_{31} + C_{41} - UxC_{13} - UyC_{23} - UzC_{33} - UC_43 = 0 \tag{3.7}$$

$$xC_{12} + yC_{22} + zC_{32} + C_{42} - VxC_{13} - VyC_{23} - VzC_{33} - VC_43 = 0 \tag{3.8}$$

The scaling of C is irrelevant so C_{43} may be set to 1. Then the above equations can be written in matrix form:

$$\begin{pmatrix} x^1 & y^1 & z^1 & 1 & 0 & 0 & 0 & 0 & -U^1x^1 & -U^1y^1 & -U^1z^1 \\ 0 & 0 & 0 & 0 & x^1 & y^1 & z^1 & 1 & -V^1x^1 & -V^1y^1 & -V^1z^1 \\ x^2 & y^2 & z^2 & 1 & . & . & . & & & & . \\ . & & & & & & & & & & . \\ . & & & & & & & & & & . \\ . & & & & & & & & & & . \\ 0 & 0 & 0 & 0 & x^n & y^n & z^n & 1 & -V^nx^n & -V^nY^n & -V^nz^n \end{pmatrix} \begin{bmatrix} C_{11} \\ C_{21} \\ . \\ . \\ . \\ . \\ C_{34} \end{bmatrix} = \begin{bmatrix} U^1 \\ V^1 \\ . \\ . \\ . \\ U^n \\ V^n \end{bmatrix} \tag{3.9}$$

Two equations result for every association of an (x, y, z) point with a (U, V) point. It is usually done using a reference object or known object with a known location.

3.2.4 Inverse Transform

Finding the world coordinates of an object corresponding to the image point relies on the fact that the perspective transformation matrix affects the z component. This information is lost when the z component is projected away orthographically, but it encodes the relation between the focal point and the z position of the point. This third component defines the distance of objects that lie on the same point in the image. The inverse perspective transform P^{-1} as:

$$(x', y', p, 1)P^{-1} = (x', y', p, 1 + \frac{p}{f}) \tag{3.10}$$

The above equation can be rewritten as :

$$(x, y, z, 1) = (\frac{fx'}{f+p}, \frac{fy'}{ff+p})'\frac{fp'}{f+p}, 1) \tag{3.11}$$

Eliminating the parameter p between the expressions for z and x and those for z and y leaves :

$$x = \frac{x'}{y'}y = \frac{-x'}{f}(z - f) \tag{3.12}$$

Thus x,y and z are linearly related, all points on the inverse perspective transform of an image point lie in a line, and both the viewpoint$(0, 0, f)$ and the image point$(x', y', 0)$ lie on it. Using a scaled C so that $C_{43} = 1$, and the world points are written as $x = (x, y, z, 1)$ and image points are $u = (u, v, t)$. Therefore actual image points are

$$U = \frac{u}{t}, V = \frac{v}{t}, \tag{3.13}$$

Since,

$$u = xC_1 \tag{3.14}$$

$$u = Ut = xC_1, v = Vt = xC_2, t = xC3 \tag{3.15}$$

Therefore,

$$UxC_3 = xC_1, VxC_3 = xC_2 \tag{3.16}$$

Which can be written as

$$x(C_1 - UC_3 = 0, x(C_2 - VC_3 = 0 \tag{3.17}$$

For any U,V in the image and camera model C, Two planes intersect to give us the desired line.

$$ax + by + cz + d = 0 \tag{3.18}$$

Assuming the above general plane equation and comparing equation 3.16 to 3.18

$$a_1 = C_{11} - C_{13}U, a_2 = C_{12} - C_{13}V \tag{3.19}$$

The direction (λ, μ, η) of the intersection of two planes is given by the cross product of their normal vectors:

$$(\lambda, \mu, \eta) = (a_1, b_1, c_1)x(a_2, b2, c_2) \tag{3.20}$$

$$= (b_1c_2 - b_2c_1, c_1a_2 - c_2a_1, a_1b_2 - a_2b_1) \tag{3.21}$$

then for a particular z_0

$$x_0 = \frac{b_1(c_2z_0 + d_2) - b_2(c_1z_0 - d_1)}{a_1b_2 - b_1a_2} \tag{3.22}$$

$$y_0 = \frac{a_2(c_1z_0 + d_1) - a_1(c_2z_0 - d_2)}{a_1b_2 - b_1a_2} \tag{3.23}$$

which can be written :

$$\frac{x - x_0}{\lambda} = \frac{y - y_0}{\mu} = \frac{z - z_0}{\eta} \tag{3.24}$$

3.3 Experimental Ecosystem

The experimental setup included the Robot modified with feedback of potion of each servo. Tracking of the centre of the robot using BEETag, via the camera which were placed at 1.2m over head. The setup was placed strategically to swap the substrates based on the requirements without affecting the rest of the ecosystem.

3.3.1 Code Execution

This is a high-level explanation of the code from the tracking video as input to the output with respect to the ground truth reference. The first step was to make sure that both cameras were recording simultaneously as any lag would lead

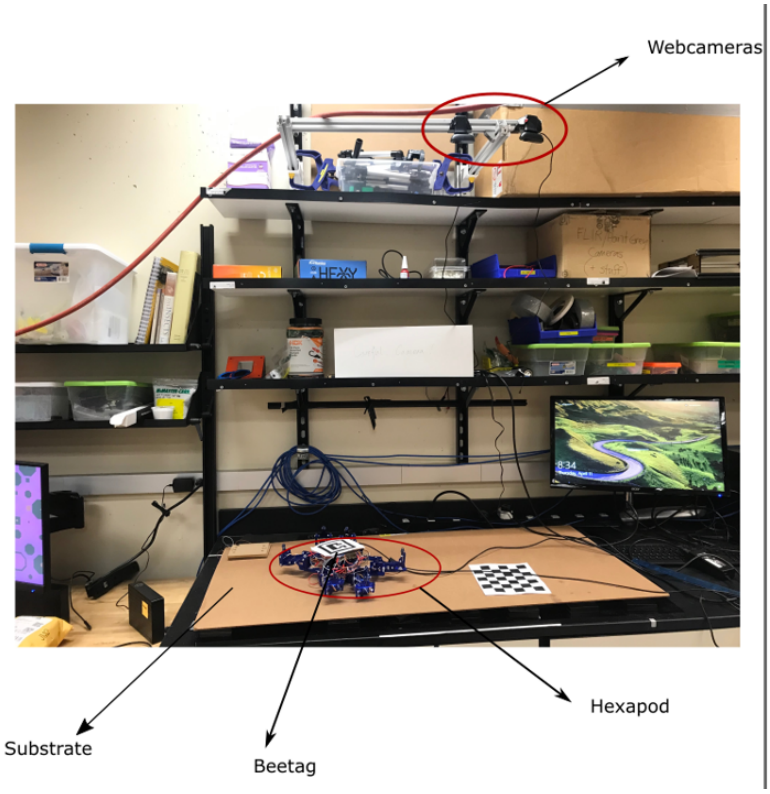

Figure 3.8: Experimental Setup of Tripod gait analysis

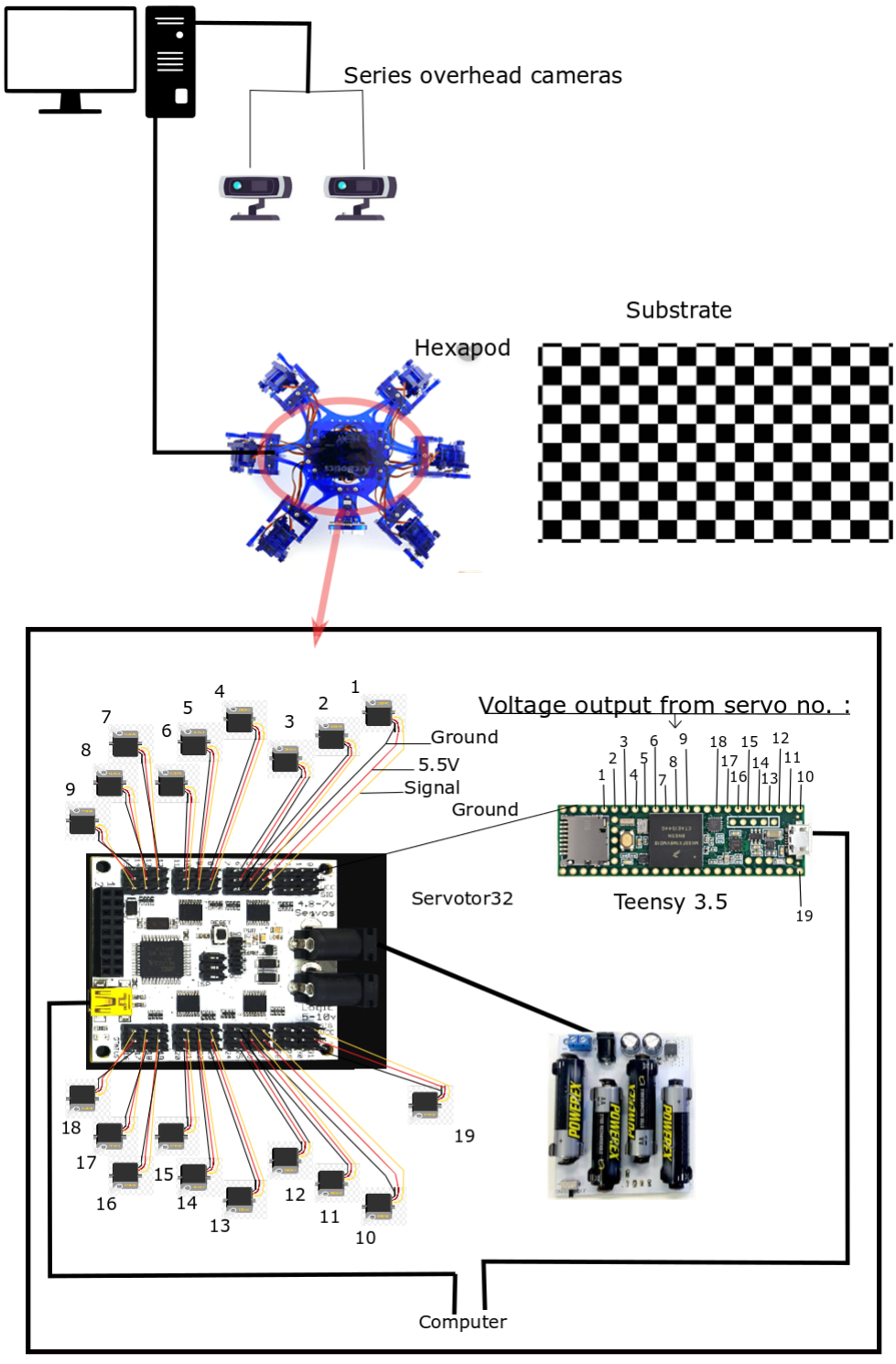

Figure 3.9: Schematic of the experimental setup

to inconclusive results. We utilized an OpenCV program that gave us access to multiple USB at the same time. Now, once the cameras recorded the videos of a run they were dismantled into their various frames and the BEETag code located the Tag and recorded the position of the tag in reference to each camera respectively. Then the data from each camera is fed into one code which references each frame form the both the cameras and traces the path of the robot in 3d space in reference to the primary camera in the stereo pair. Now using Inverse Transformation we converted the data of the path traced point by point to a ground reference which was the right bottom corner of the track.

3.3.2 Experiments

To test and compare the performance of the robot across the different substrates we performed 40 runs per substrate to get a reasonably dependable data set. To randomize the possible outcome of the trials the robot was placed at different starting positions. Also, Each servo was coded to start from the centered position i.e 0Deg. This added another layer of randomness to the robot. This played an important role since in some trials the robot did not start absolutely parallel to the leading edges of the obstacles, which helped us study the reaction of the robot and the gait to self correct its trajectory in an open loop system. Since, the robot was coded to always begin with the left tripod stepping forward first. It helped Prevent any bias during the first point of contact the robot made with the rough surface. In some runs the robot would turn due to the effect of a leg getting stuck and not realign itself with the central axis of the track and ultimately veer off the track sideways. In such cases a tolerance thickness of 1inch was considered from the side of the track. Due to this the duration of each run was inconsistent. Therefore, we chose the stride length as a common parameter to compare across all runs. The robot could run for 2hours till the batteries were completely discharged from a full charge. To avoid any performance degradation over time due to voltage drops, experiments were performed in intervals of 20 minutes between which the batteries were recharged. The setup had an overhead light source which occasionally would be reflected by the BEETag leading to missing frames of data. In such cases if

the missing frames were more than 30 in a row i.e 900 seconds of data, that run was not considered. In runs with less than 30 frames in a row missing we used Bi-linear Interpolation. As mentioned above to avoid inconsistency across runs Stride length was considered the common factor to compare the performance of the robot. Therefore, it was essential for us to mark the beginning and end of each phase of the legs(Swing + Stance). Due to the randomness of the trials time directly could not be the marker. Ordinarily, a digital high and low pin is used. But in our robot the distribution of the signal input and the voltage output into two different micro-controllers denied us the possibility to digitally mark a high and low pin. We used another servo and set it to sweep its entire range of motion forwards and backwards simulating a high pin signal. We setup a master code which set in motion all the components of the experiment when executed.

3.3.3 Data Flow

The master code once executed in python simultaneously initiates three codes, the input for the robot's servos, the output from the potentiometer of each of the servos and the tracking code to trace the path traveled by the robot. The output from each of the events are then simultaneously recorded and stored into a folder, which is fed to the MATLAB user interface for further processing.

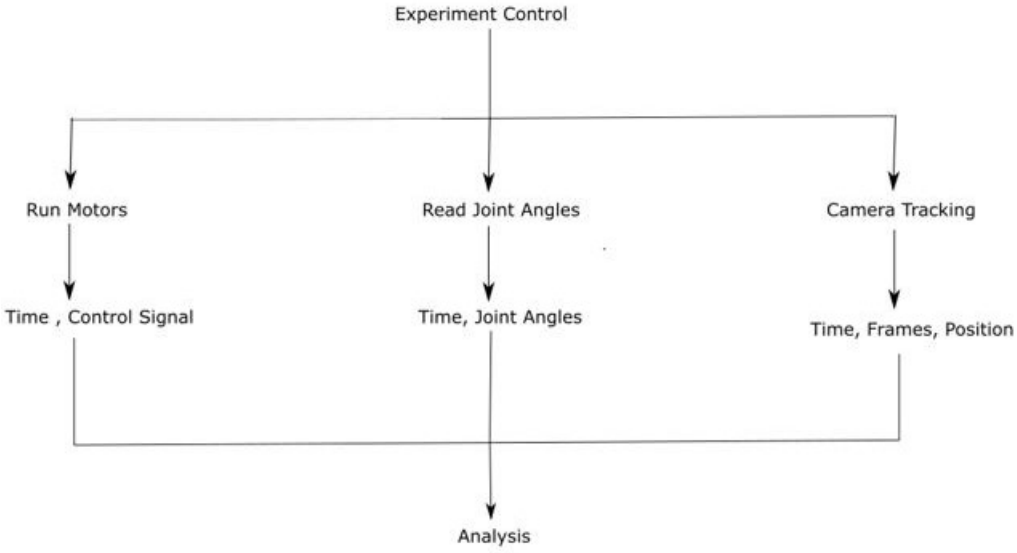

Figure 3.10: The different streams of data collection during experimentation taking place simultaneously

3.4 Servo Position Analysis

3.4.1 Voltage output from Servos

This is the output of the voltage varying in accordance to the angular position of the servo marked by the potentiometer. Each trough and peak is representative of the beginning and end of the swing phase respectively. The plot has flat sections of voltage both before and after the sinusoidal inputs. This is the effect of the way the master code was written. The code runs for a fixed duration to limit the total number of frames as beyond a certain number the data set becomes too large leading to very slow computation. Each of the data points have a time difference of 5ms. The servos were set up in parallel but there were some losses which lead to tripod two having a slightly lower value registered. This was a very insignificant drop in voltage to affect the performance of the robot.See figure 3.11

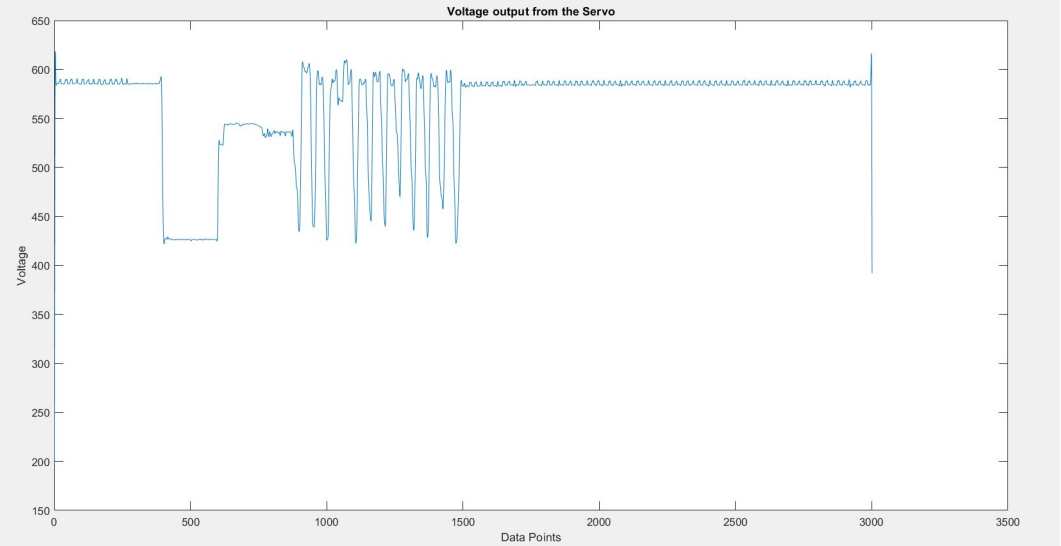

Figure 3.11: Voltage output from the servo

3.4.2 Stride identification

As mentioned above, we used an additional servo to mark the beginning of each stride. Which, was overlaid on the servo voltage output from the Left front leg of the first tripod. This was necessary because the servo was programmed in phase with the first tripod. Our paper was more geared to focus each interaction with the obstacles in a run. To be able to understand the nature of the occurrence, the instant that it took place at was crucial therefore, we studied each stride separately. The trigger servo was coded to sweep its complete range before the first signal was given to the tripod one. To compensate for this the code was setup to pick up the peaks of the trigger servo and add 2 data points to the x axis position of the peak. As we can see in the figure the first peak of the trigger servo is highlighted. See figure 3.12

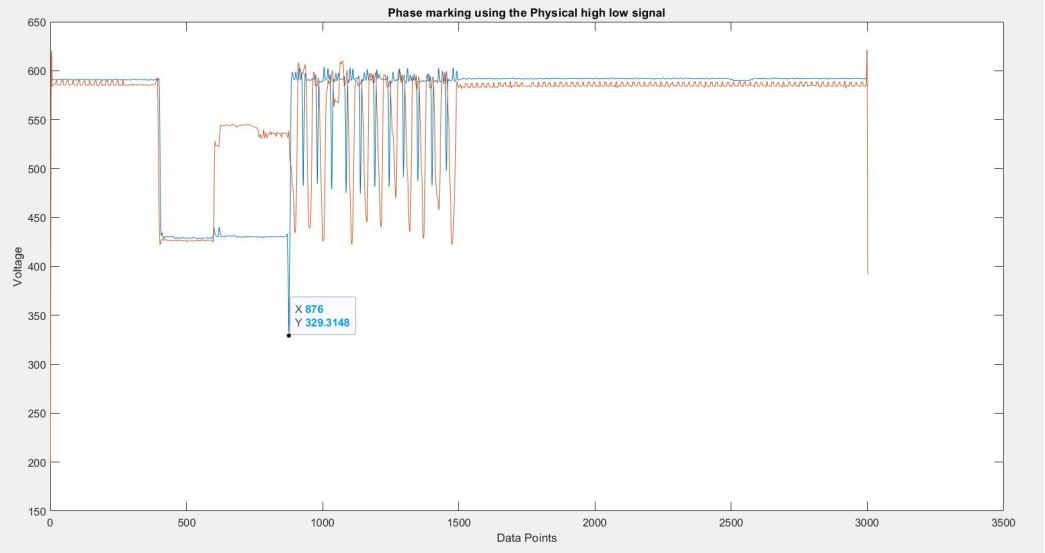

Figure 3.12: Using the voltage output from an additional servo to mark the beginning of the each phase

3.4.3 Comparison of two tripods

The first thing we needed to compare was if the difference in the recorded voltage values actually represented a difference in the performance across the two tripods. To avoid any issue we normalized the voltages. comparing the amplitude and the frequency across the two tripods we plotted the Front, middle and hind legs respectively.Tripod one constituted of the Left Front leg, Right Middle leg and the Left Back Leg. Tripod two constituted of the Right Front Leg, Left Middle Leg and the Right back leg. The two tripods were actuated alternatively which lead to the stability of the Gait. This plot represents the phase shift between the two tripods in each of the front, middle and hind legs respectively. The two x and y axes are time in Seconds and the combination of the legs being compared respectively.In this high level comparison we can already observe a break in the phase of the right front leg due to the interaction with an obstacle. This reaffirmed the use of the hip joint as a phase representation of the entire leg. For different runs the number of strides varied. There are multiple reasons for such differences. The best case is when the robot walked on the flat substrate and maintained a constant velocity throughout the run. although, even on the flat substrates

the robot could experience slipping which lead to an increased no. of strides to complete the same distance. Taking into consideration all the variations on the flat substrate a benchmark was set. Using the set benchmark the runs on the simulated rough substrates were analysed. The two possibilities were that the no. of registered strides were less or more. The reasons for the strides to be less than the benchmark were either the robot veered off the track or the robot got stuck and we concluded the experiment. The reasons for the strides recorded to be more than the benchmark were if the robot encountered an obstacle and either got stuck temporarily and then recovered or that the robot did not follow a straight line of motion. In such instances we had to compare the signal data with the tracking data to establish if the robot was successfully able to cover the distance of the track. As in some instances the robot would run out of time. In the figure 3.13 we can see that the robot's left front leg got obstructed by an obstacle in the 4^{th} stride.

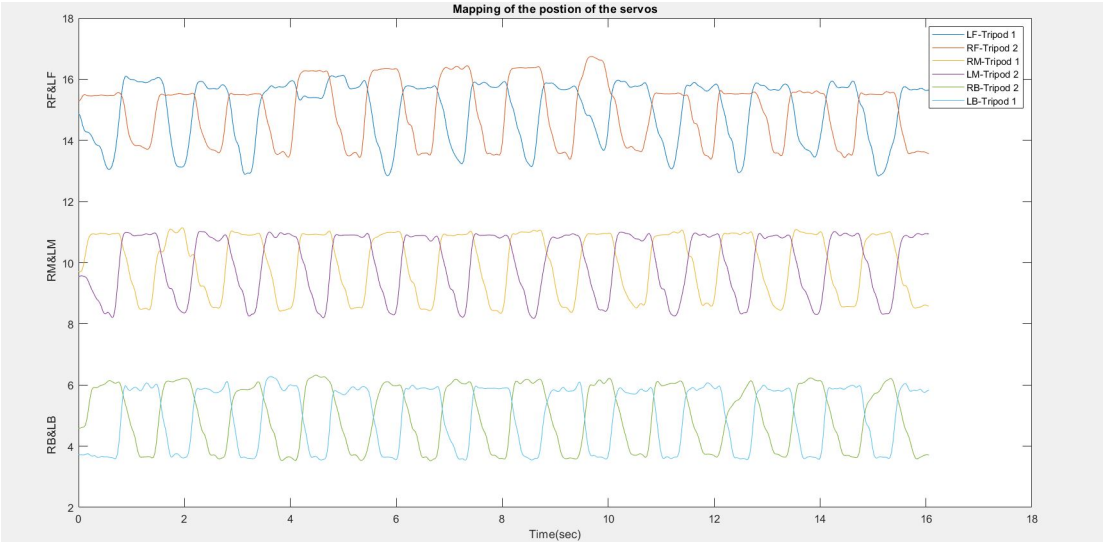

Figure 3.13: Plotting the voltage outputs of the six hip joints representing the phase of each leg.

3.4.4 Identifying the Peaks

Once each stride was identified, we needed to identify the position of the servo both at the beginning and the end of the swing phase. This was crucial to identify the nature of interaction of the leg with the substrate. We needed to study the peaks and troughs separately as an obstacle would prevent the leg from reaching the desired position. We needed to know the occurrence of the interaction with the obstacle to further study the correlation of the event with the effect on the entire robot. As we can see in figure3.15 the leg gets lodged into a possible crevice at the end of the previous swing and therefore cannot sweep back to the other end of its range of motion. Combining such features from all the legs and with the video output data we can study how the robot reacts to such situations.In Figure 3.14 and 3.15 we can observe how the leg was not able to make a complete sweep in the 4^{th} stride due to an obstacle.

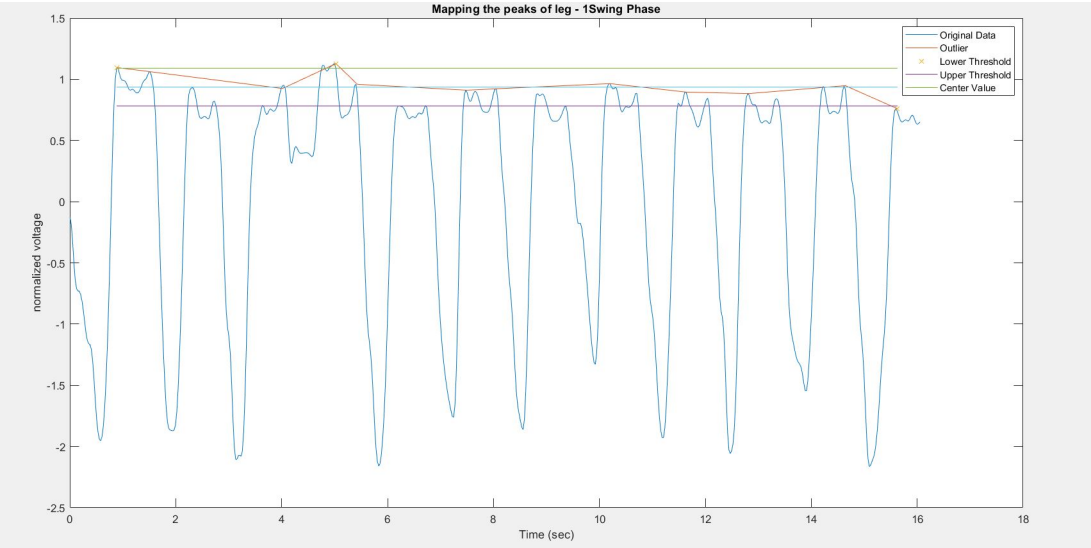

Figure 3.14: Marking the peaks at the end of the swing phase

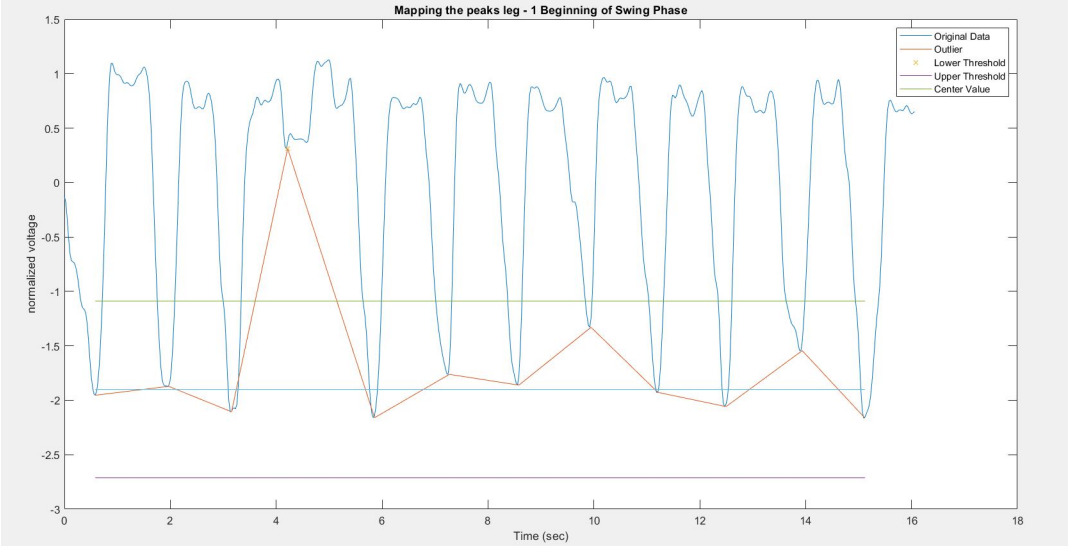

Figure 3.15: Marking the peaks at the beginning of the swing Phase

3.4.5 Comparing the performance across all substrates

After marking the peaks and troughs across all substrates we then plotted all the points to compare the performance of the robot across all the substrates. Each segment in the plot is a focusing on the behaviour of each leg on the different substrates. The first box in each section are runs in air to record the true signal of the robot. Ideally the performance of the robot in air and on flat should be the same, but in some cases the robot experienced some slippage due to the contact with the substrate. The order of the last two boxes are arranged based on the variance. The variance in most cases were larger in the 3inch substrate in comparison to the 5 inch substrate. Therefore, we plotted the 5 inch before the 3 inch to maintain the inherent trend of growing variance. Along with the analysis of each leg across the different substrates we also wanted to see if any trend appeared across the different legs of the robot. Depending on the position of the leg if some legs faced more obstacles than others. The axes are Position in Degrees the name of the leg being observed. These gave us a clearer picture of the difference in the way the robot was interacting with the substrates. Also, brought to our attention the higher variance in the data recorded by the front and middle legs on an average

when compared to the data collected for the hind legs. This motivated us to find a possible correlation of such a feature in real six legged insects too. See Figure 3.16 and 3.17

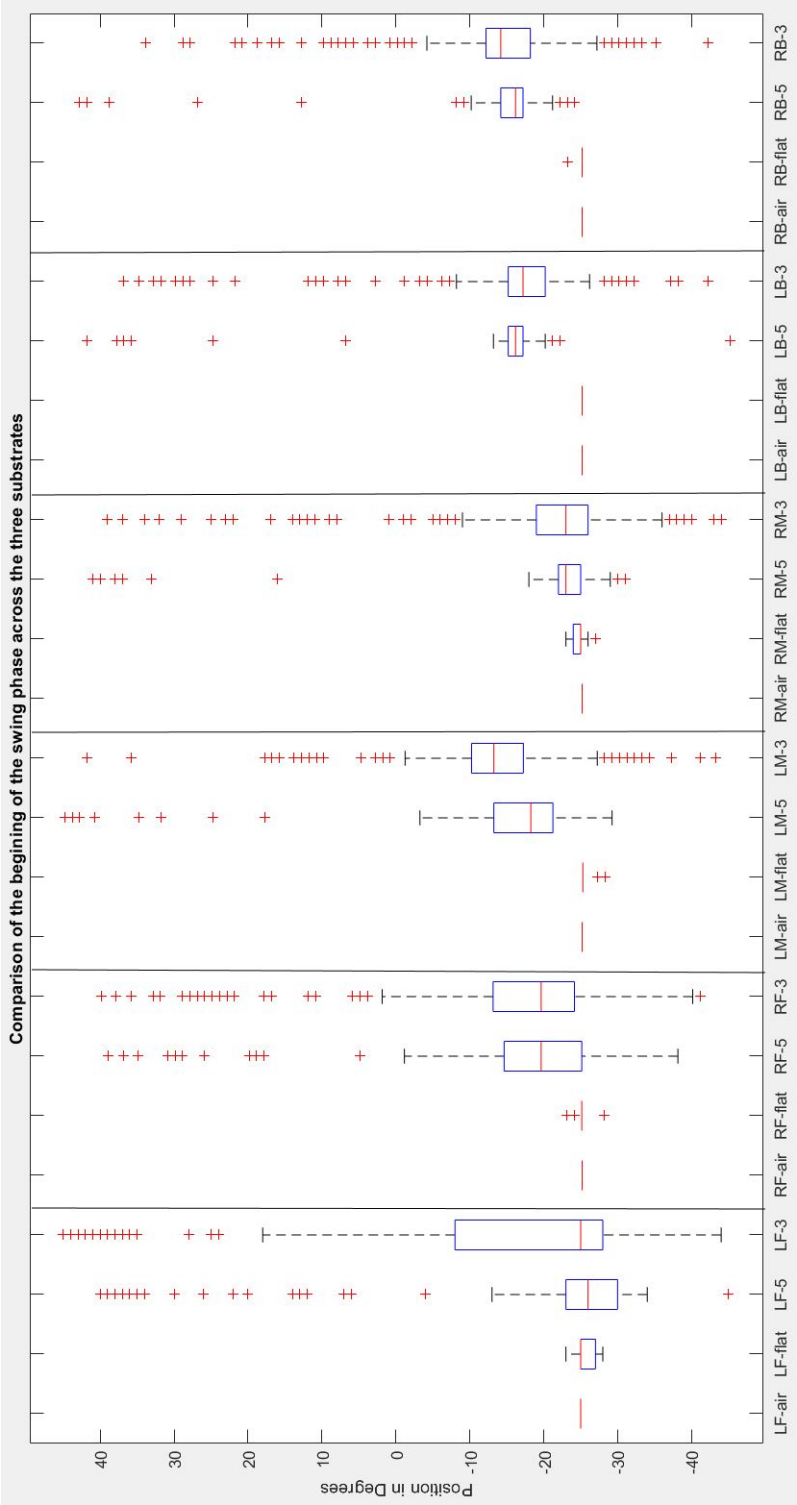

Figure 3.16: This plot is the combination of all the data from the legs from the runs on the different substrates marking the different positions reached after the beginning of the swing phase.

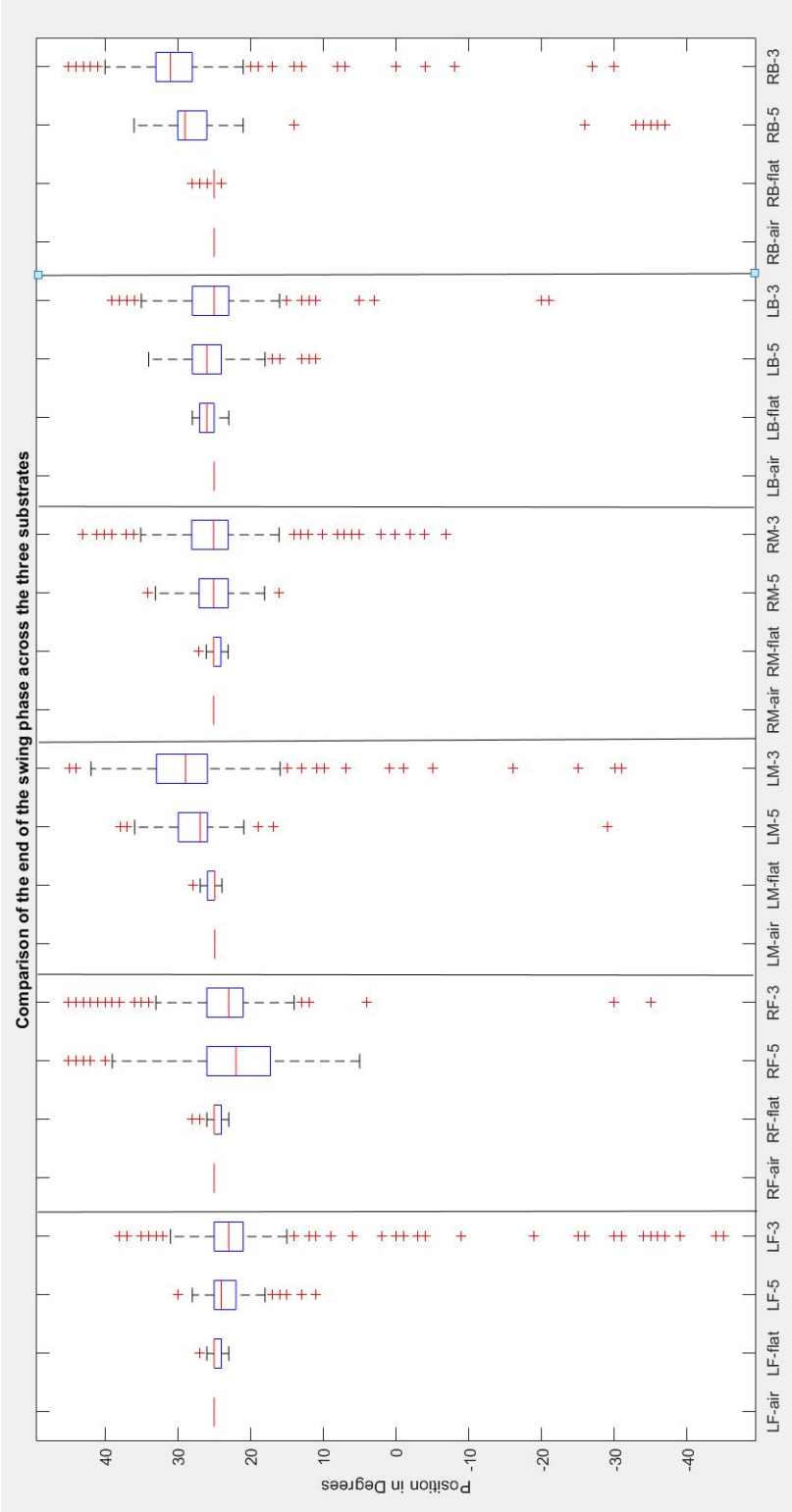

Figure 3.17: This plot is the combination of all the data from the legs from the runs on the different substrates marking the different positions reached after the end of the swing phase.

3.4.6 Frequency of interactions across all substrates

The box plot does give us an idea of the quality of performance of the different legs based on their position, but can be misleading . Boxplots marks the median of the runs, where the data in the rough substrates can be biased due to large no. of interactions with obstacles affecting the standard deviation and the variance of each distribution. We used an inbuilt function in MATLAB called boxplot to plot the angular positions. This function is focused around the mean of the data which can vary depending on the distribution. Therefore to truly support our hypothesis we needed to study the frequency of interactions with the obstacles in the rough substrates. Using the same peak position data but representing it in a histogram form gives us an idea of how often the desired position was not achieved. The plot below marks the max and min angles swept by the servos marking the beginning and end of the swing phase. In these we can see different behaviours of different legs depending on the position of the leg in relation to the direction of motion. Each plot is a compilation of the peak and trough angles reached by the respective legs in different substrates across all the recorded runs. See figures 3.18, 3.19, 3.20, 3.21, 3.22, 3.23. Although, the box plots give us a qualitative analysis of the performance of the legs, the histogram gives us a quantitative analysis of the performance of the legs. Using which we can correlate the data with the video outputs to see how the robot reacted to each interaction.

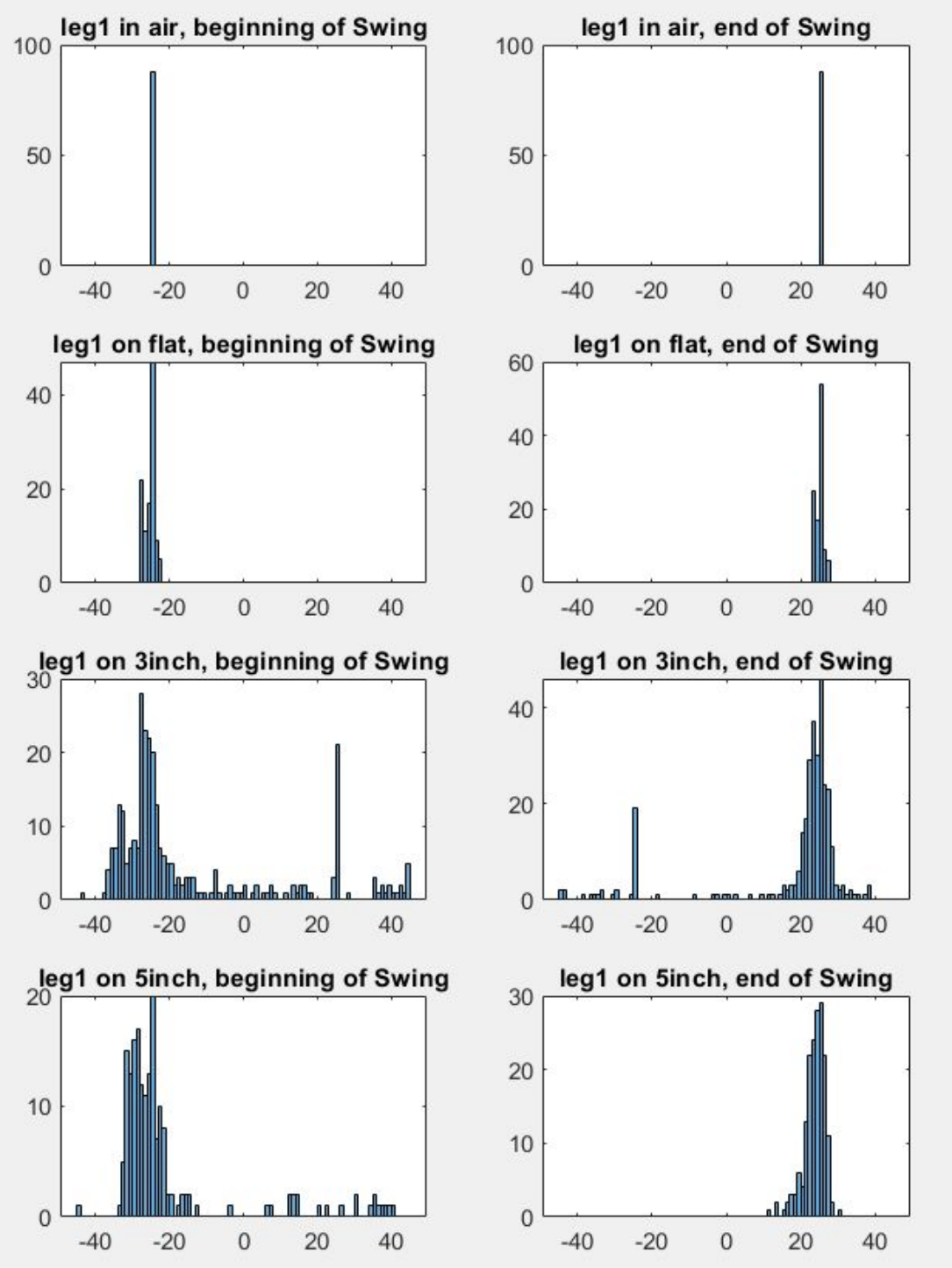

Figure 3.18: Frequency of interactions of leg 1 across all substrates

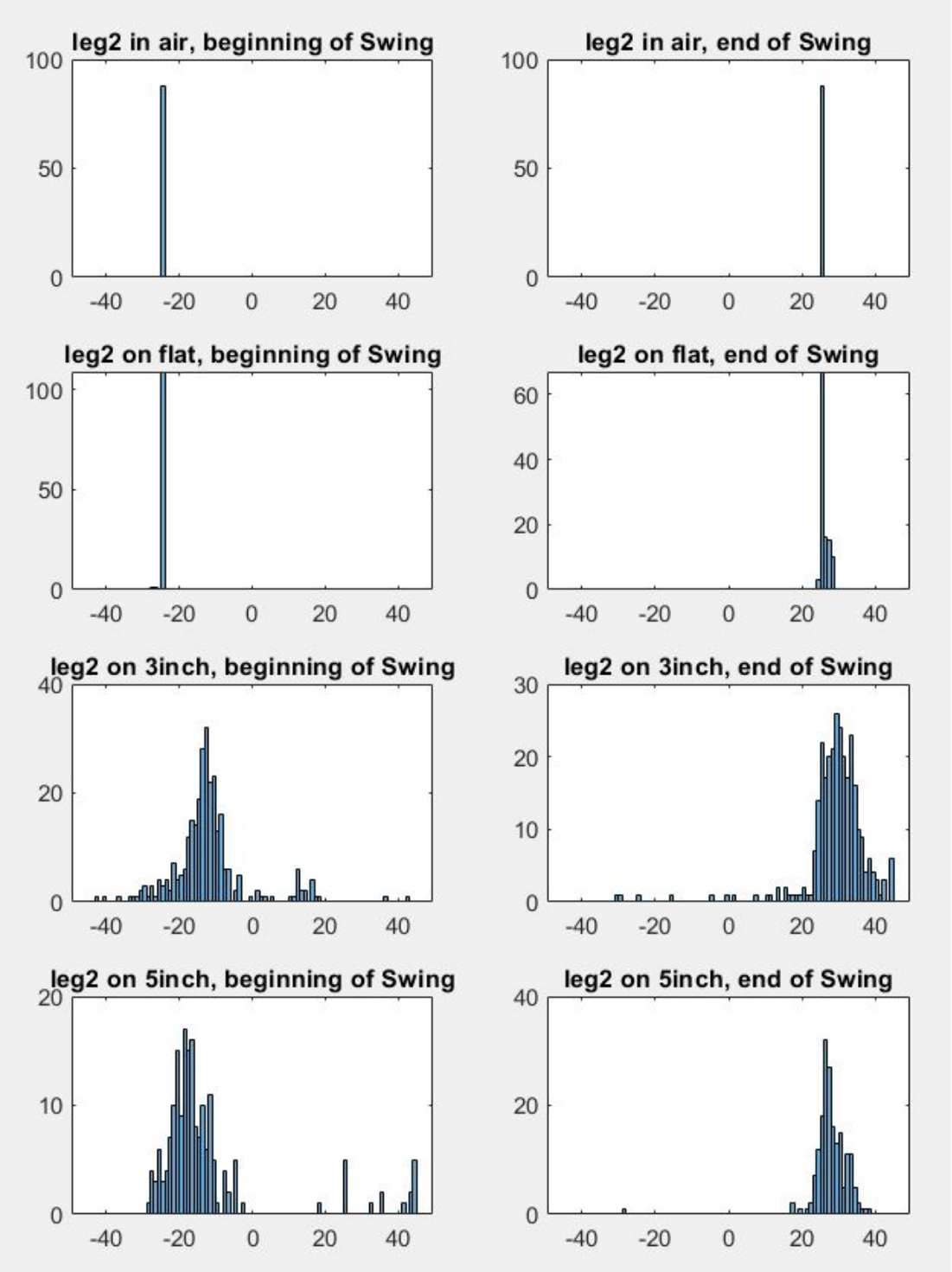

Figure 3.19: Frequency of interactions of leg2 across all substrates

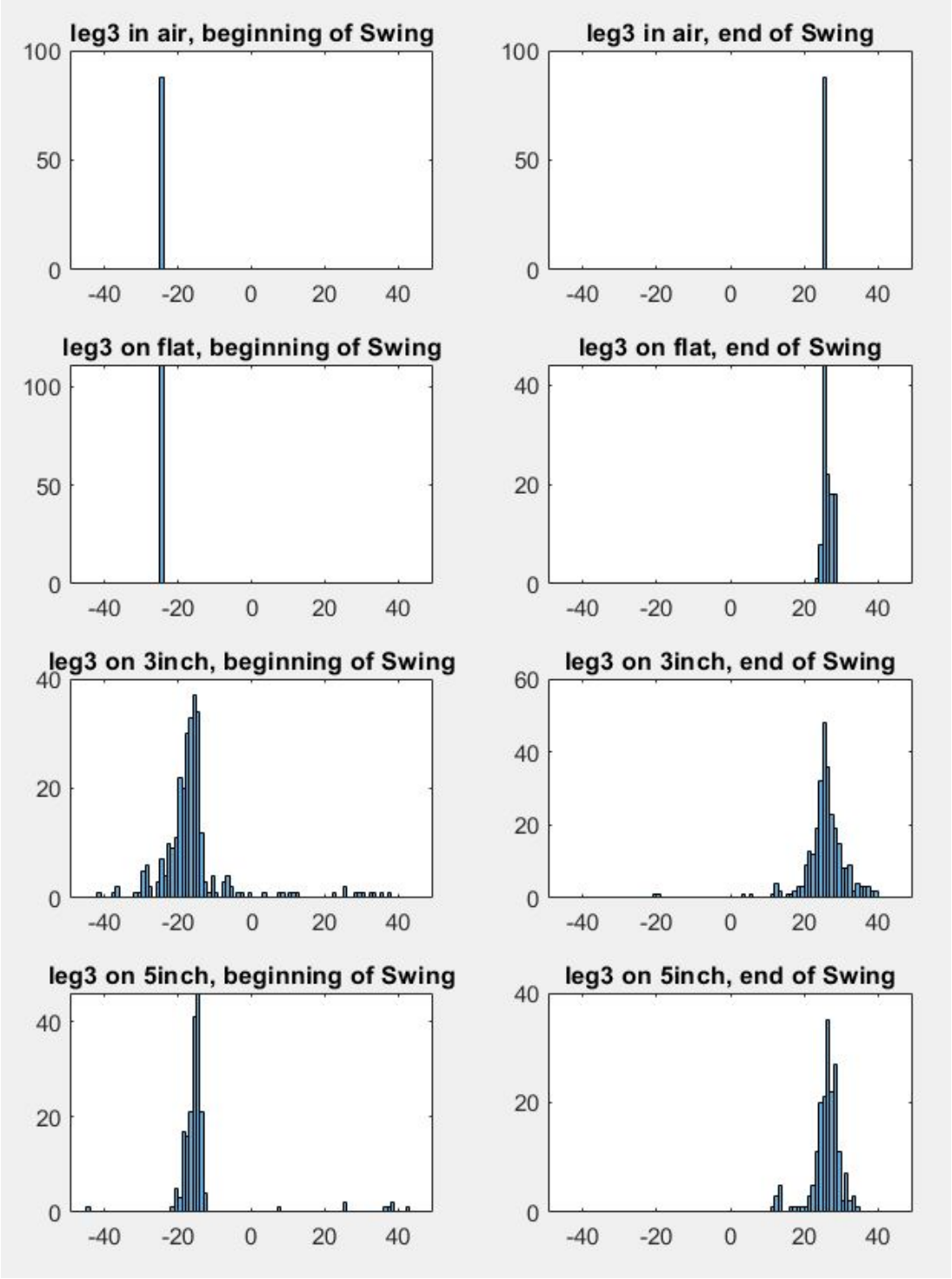

Figure 3.20: Frequency of interactions of leg3 across all substrates

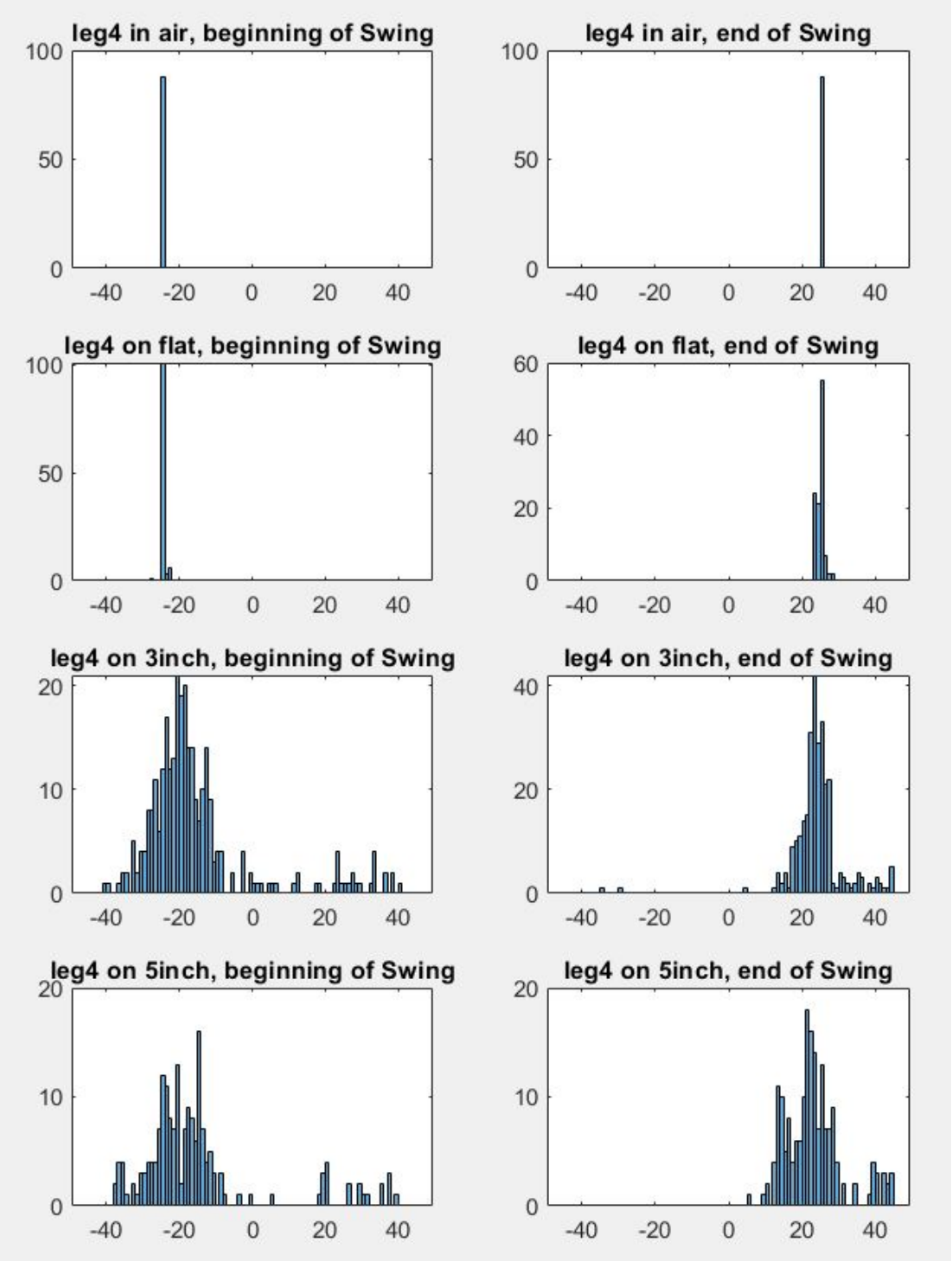

Figure 3.21: Frequency of interactions of leg4 across all substrates

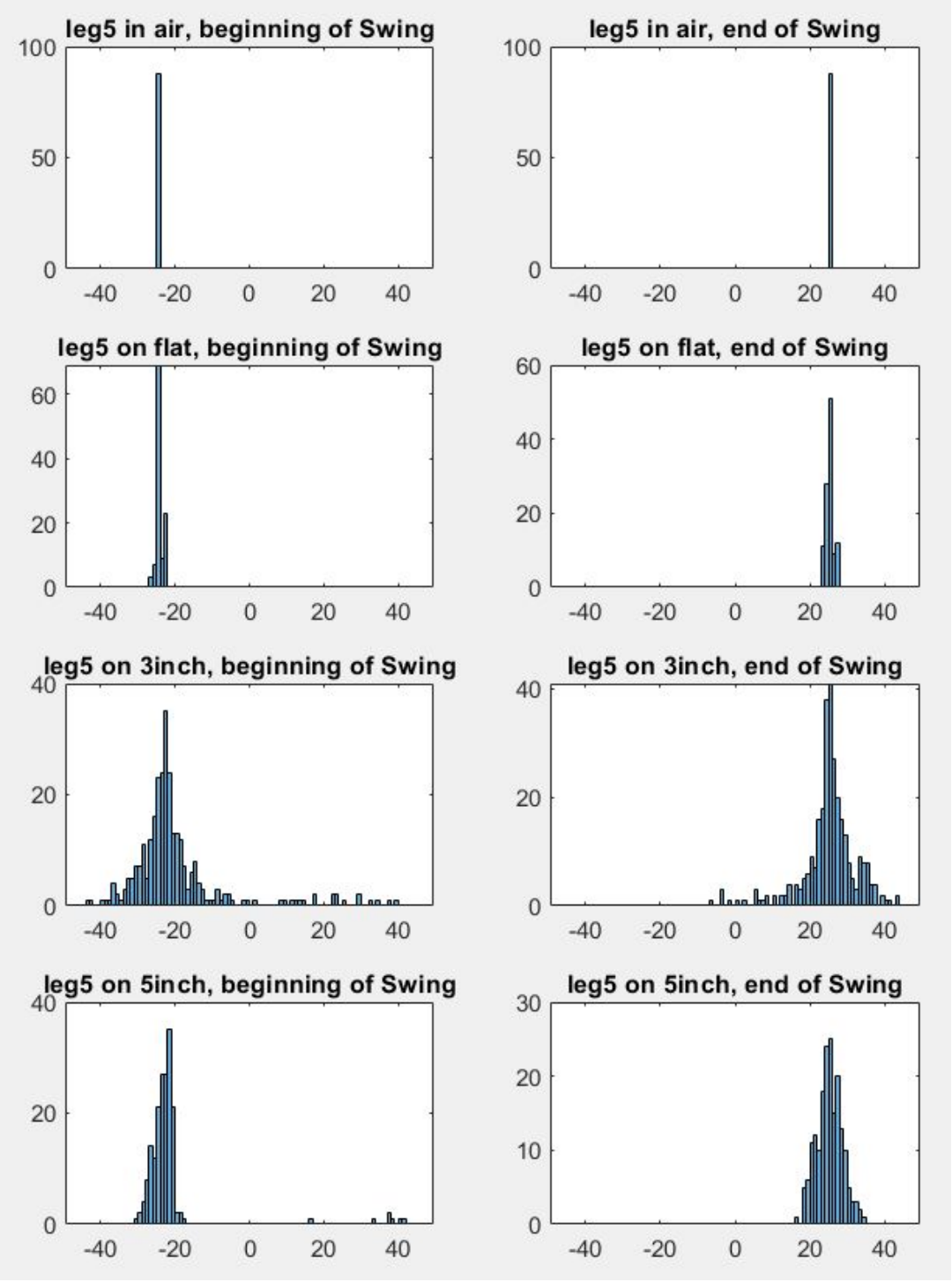

Figure 3.22: Frequency of interactions of leg5 across all substrates

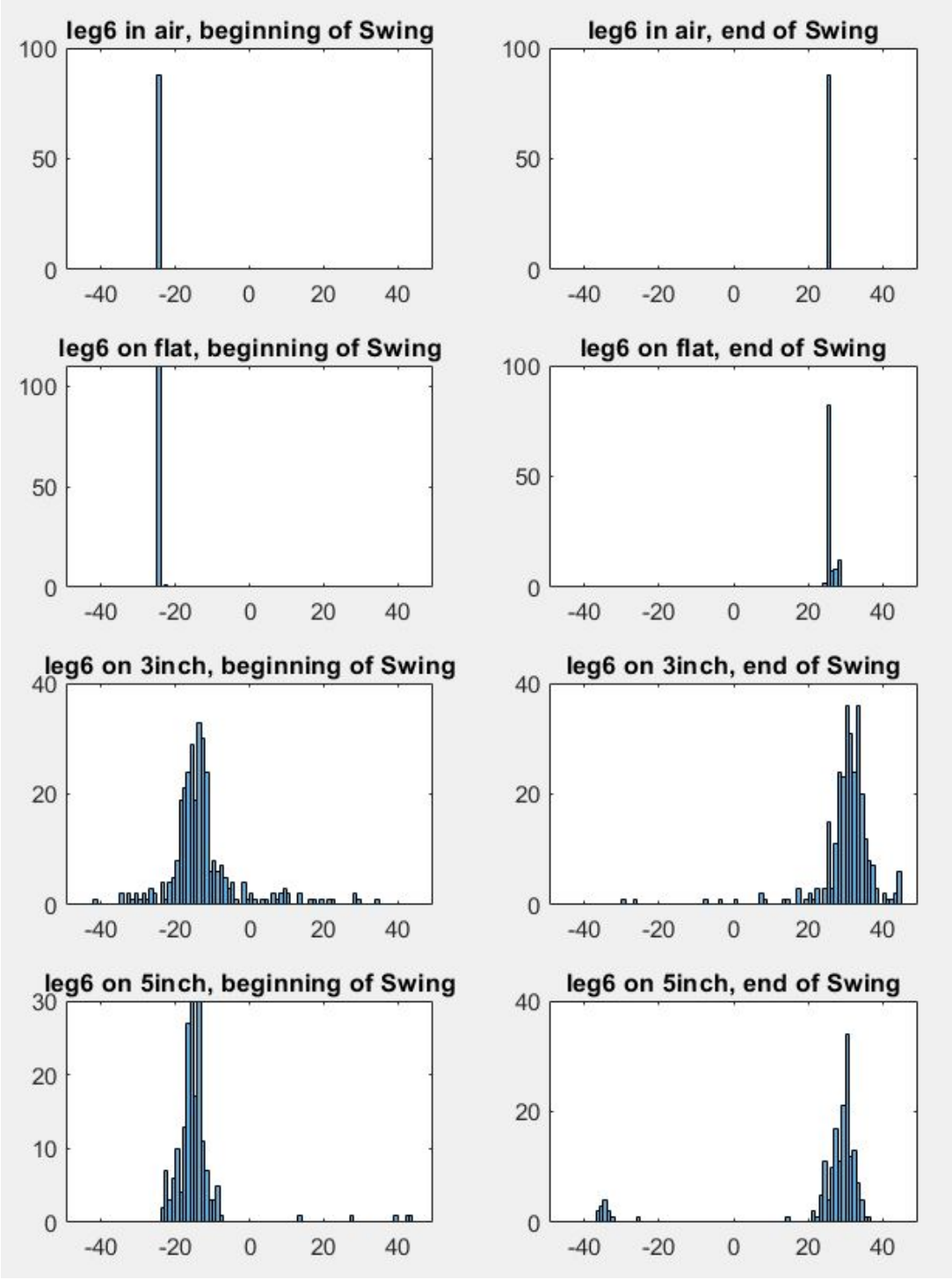

Figure 3.23: Frequency of interactions of leg6 across all substrates

3.4.7 Summary of Analysis

Legged robots are able to propel themselves by their legs, this is the outcome of the forces acting on the legs due to the contact with the ground. In the case of hexapods there are different patterns in which the robot can order the movement of their legs to move in a particular direction. The most commonly used gaits observed in nature are Tripod Gait, Quadrupedal gait, Wave Gait, random Gait and in some cases even Bi pedal Gaits [4]. The use of the different gaits by hexapedal runners depends on many factors like: the type of surface they are traversing, the incline of the surface, the speed at which they are travelling, the amount of additional weight they are carrying etc. Over the years through extensive studies of such six legged insects, it is a common and reoccurring conclusion that, when travelling on planar surfaces with no incline and at a moderate speed Tripod gait is the most commonly used gait. Following the conversation and with our goal in mind we chose to analyse the performance of a hexapedal robot using the tripod gait. Now, returning to the initial point of the forces acting when a robot propels itself. The benefits of legged motion over wheeled motion is that legged motion provides control over both the horizontal and vertical forces acting. These forces move up the legs and ultimately affect the joints attached directly to the main body. This is the reason why many underactuated (6DOF) robots exist and can perform equally well and in some aspects even better than 18DOF or more robots. Kinematics and dynamics play a crucial role when studying the movement of any body in space. The kinematics of a design can be affected by the dynamics it faces on application. This inter-relation of dynamics and kinematics and the effect of the force being realized at the hip joint led us to use the hip joints as the phase of the entire leg. The idea that any force experienced at any segment of the leg will ultimately show itself as an angular deflection at the hip is primarily what the initial part of our experimentation is focused on.

Using the voltage output of the potentiometer of each servo we intended to study the reaction of each leg. The results that we collected revealed a trend across all the substrates. In both the boxplots and the frequency plots it was clear that the most no. of obstacles were faced by the front legs and occasionally the

middle legs. Now this prompted us to question if such a tendency was visible with real insects or not. Two blaring conclusions are revealed. First, the ability of the insect to probe and decide a path before placing the foot down.Second, the flexibility of the legs due to 7DOF of their inherent design, where the leg can conform around obstacles and be placed beyond it. Now, it is hard to understand of all the observed instances where an insect crosses an obstacle if it were a choice or if it were due to the physicality of the legs design. The first conclusion has been tried and tested, where neural networks are implemented to improve the decision making process of the robot. The second conclusion focusing purely on the physicality of the event is still not as well explored. This led to our hypothesis of testing the possible improvement of the performance of our open loop robot across rough substrates with a compliant leg design.

3.5 Tracking Data

3.5.1 Instantaneous Velocity

The position data provided us with evidence of the interactions but was limited to the local system of the leg. It was crucial to understand the effects of the interactions at the level of the entire robot. This parameter further analysed the higher level behavior of the open loop control robot on the substrates. The robot had a slight oscillatory tendency when taking steps. The instantaneous velocity of the center of the robot provided us with a quantitative value of the difference between the nascent oscillation and the oscillation induced due to the obstacles.These plots give us a clearer picture of the slightly oscillatory movement of the robot and magnifies the response to an interaction. This reinforced the need of compliant legs for application where there is need for a high payload. The combination of these plots from every run and the angular results of the robot's servos led to a clearer picture of self stabilizing nature of the tripod gait. Which emphasised on our hypothesis were the performance of tripod gait can be significantly improved by the addition of compliant leg designs. In Figures 3.24 and 3.25 we can see the instantaneous velocity of the robot from a run on a 3 inch

substrate, on comparing the plots to the figure 3.13 we can see that the effect of the front leg getting obstructed in the 4^{th} stride led to a lateral shift in the path of the robot. Which can be observed as a peak around the 150^{th} data point in 3.25 and a flat region in the 3.24.

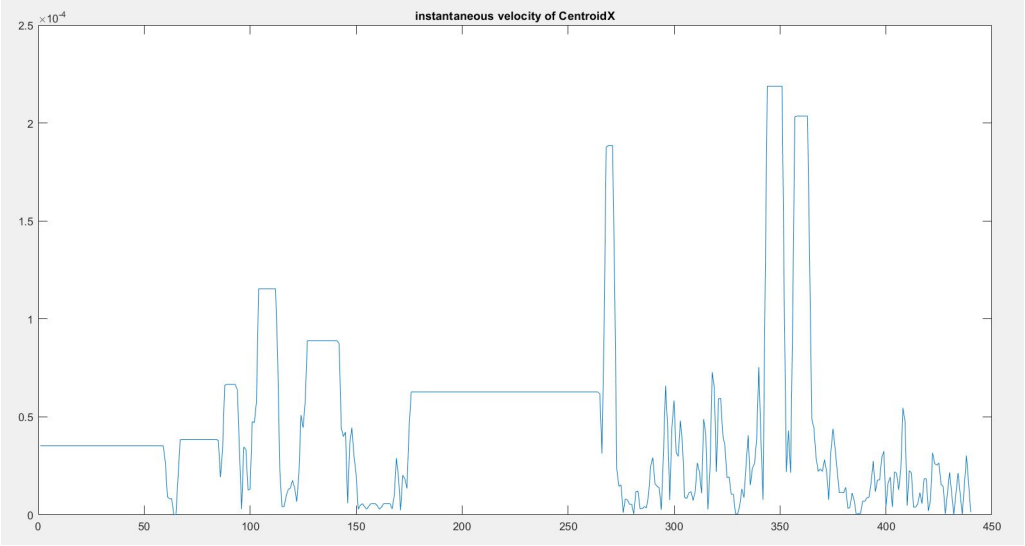

Figure 3.24: Instantaneous velocity of the robot in the X Direction

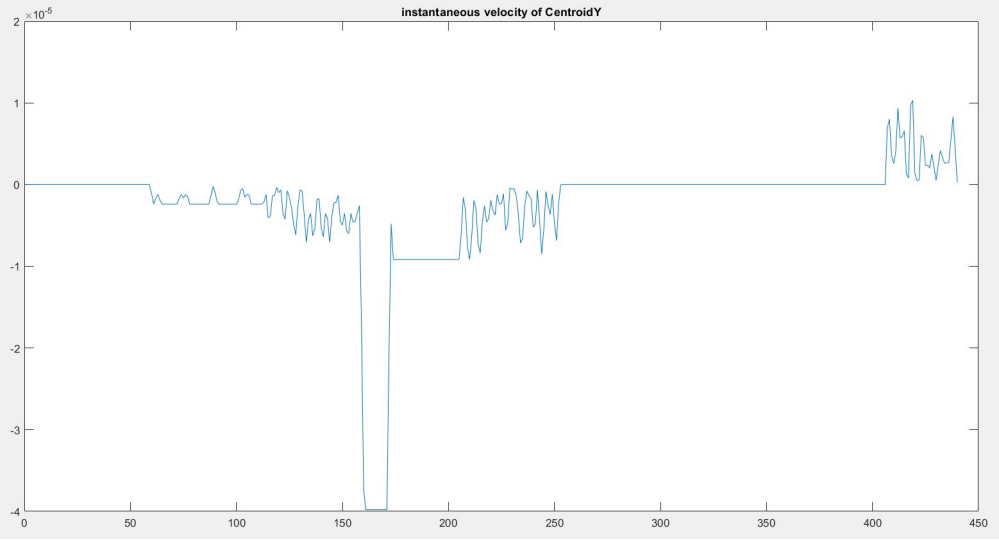

Figure 3.25: Instantaneous velocity of the robot in the Y direction

3.5.2 Distance per stride

As mentioned in the experimental setup chapter the distance per run is not consistent as the robot in some instances would veer of the path parallel to the axis along the length of the track. Therefore we needed to find a common factor which is the distance per stride. See Figure 3.26

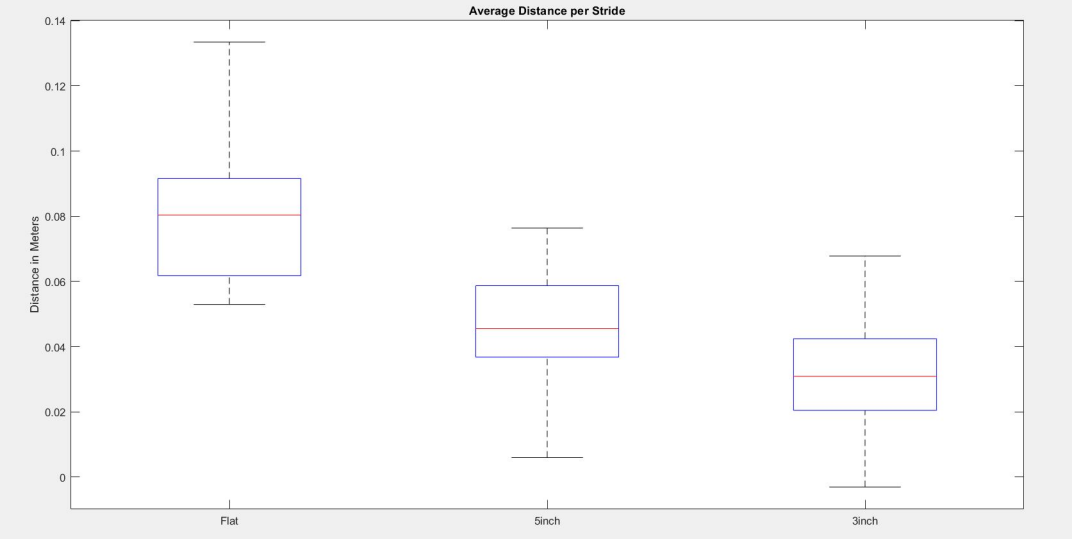

Figure 3.26: Average distance covered per stride across all substrates

3.5.3 Summary of Analysis

Although the goal of the project was now to study the interactions of legs with obstacles. We return to the same point, that the forces from each leg are ultimately realized at the hip which is directly attached to the body. Therefore, to improve the possible interaction of the legs with obstacles it was crucial to observe the entire robot. Tracking the movement of the robot across each substrate, studying the distance covered, speed and behaviour in general helped us realize that even though the desired movement of the robot is forward in a straight line, obstacles can impede the movement from any direction. This gave rise to idea of an omnidirectional design to the compliant leg. While testing with the solid legs the robot in many instances was able to realign itself to the previously defined path. This proved the stability benefits of the tripod gait. On finding the correlation between the servo

position data and the tracking data we observed a possible relationship between the stride length and the size of an obstacle. The higher number of interactions of the legs with obstacles in the 3 inch substrate vs the 5 inch substrate does not seem to be a feature of the design of the substrate. Where we can simply say that as more number of blocks exist hence the more the likely hood of interaction with one. This seems to be an effect of the stride length and the presence of the obstacle at a particular instance of the swing of the leg. Both the box plots and the frequency plots revealed an inconsistency in the no. of obstacles crossed when at the beginning of the swing and at the end of the swing. This can be hypothesised to the concept of direction of driving force. Most bio-inspired robots are programmed to recoil the leg first and then move forward and then unpack the leg. When this is performed at slightly higher speeds this initial trapezoidal input signal tends to conform into a sinusoidal wave. In which the first half the amplitude is rising and the second half the amplitude is dropping. This helped us design the testing rig for the comparison of the performance of the compliant leg to the solid leg. Where along with the goal of the robot to traverse a higher obstacle, we also wanted to study the effect of the stride length on varying heights.

Chapter 4

New Compliant Leg

4.1 New compliant leg design

The first phase of the project we analyzed the performance of the robot with rigid legs on different substrates to study the influence of interactions with obstacles. Based on the results we wanted to focus on the occurrence of the interactions since we hypothesized that the performance of the robot can be improved if we reduced the instances of the robot getting stuck on obstacles. Although, the aim was to achieve this improvement by maintaining passive control of the robot. Therefore, we applied the concept distributed mechanics and came up with a design which allowed omnidirectional displacement in the robots leg. We decided to make a retrofit design so that differences from the initial robot remain low. To accommodate the elastic component and other parts of the new design the dimensions were altered a bit. The original leg hip = 26mm. thigh = 49mm, foot = 52mm. The new leg had the same hip and thigh but the foot was modified to a new uncompressed length of 111mm.

The design of the foot incorporated two directions of motion: 1. Rotation around a certain joint 2. Prismatic compression The design of the foot was an iterative process. We resolved the issue of the leg getting stuck in corners or legs unable to complete their swing to the desired position with an elastic ball socket joint. On the implication of a non-axial force preventing the movement of the leg in either the swing or stance phase the foot was able to conform around the

Figure 4.1: New Foot design with 30Deg of compliance

obstacle by not affecting the phase of the entire leg. Although, with the first iteration there were chances of the robot losing stability while walking. And in some instances, depending on the distance form the obstacle the foot would not recover to the original orientation leading to a compromised stance. To tackle this issue, we changed the design such that upon axial loading of the leg the leg would get compressed and fit into a conical shape to force the leg to retain the upright position. This modification did show promising results in both static and low speed tests.

To accommodate the ball socket, Linear spring and conical socket the length of the foot changed from 52 mm to 107mm. To compare the performance of the new leg with a comparable rigid leg, we fabricated a rigid foot of the same length and maintained the radius of the tip of the foot the same. The flexible foot was fabricated using a PRUSA mk3 and the rigid foot was fabricated on a MakerBot. We used two different printers because the finish on the flexible leg was crucial to reduce the friction between the surfaces and to prevent any unnecessary loss of

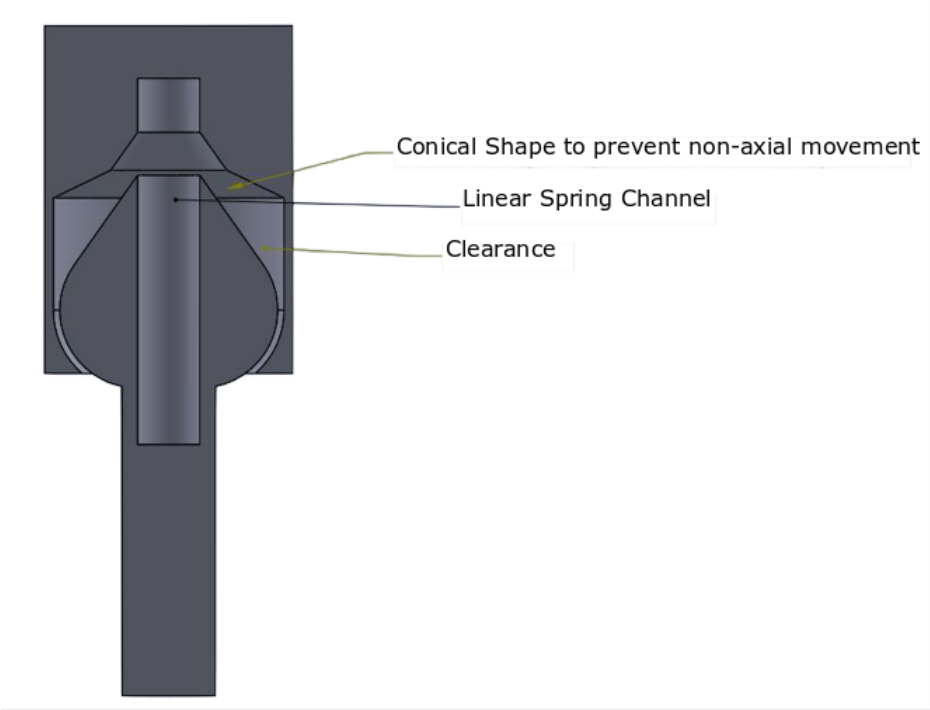

Figure 4.2: Cross-section of the New Leg Design

energy. The ground clearance of the robot changed due to the new designs. So to maintain similar kinematics we used the same DH variables that we had gathered in the original design. This was successful in our case since the foot met the ground perpendicularly and once the length of the leg changed it did not change the axis of rotation or the plane. Only the torque needed to move the leg was more due the added weight and the increased lever length.

4.2 Compliant Leg Testing

With the results of the tripod gait analysis experiments supporting our initial hypothesis of the impact of no.of interactions during a run to the performance of the robot. We needed to focus purely on the interactions and the difference in the success of the leg designs to cross an obstacle, while eliminating all other components from the previous experiment. Our goal was to establish a relationship between the stride length and height of obstacle faced, and simultaneously compare

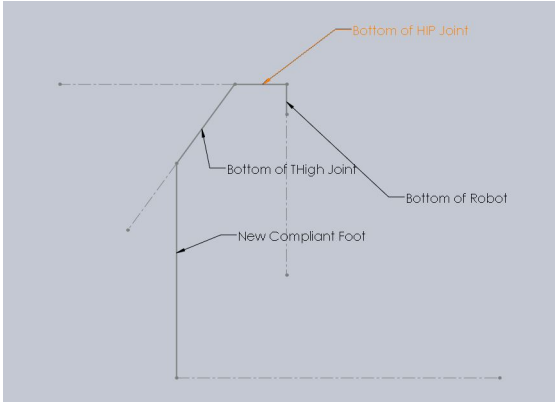

Figure 4.3: Specification of robot stance with the new leg design

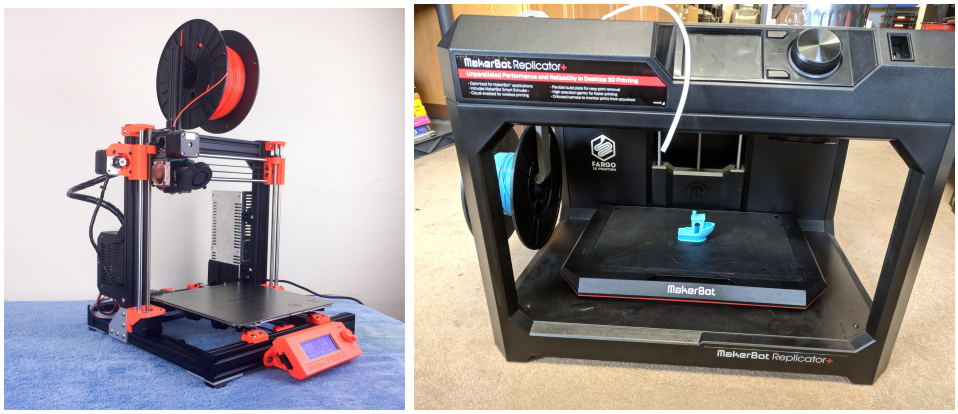

Figure 4.4: Prusa i3 mk3 3d printer used to fabricate the new complinant leg design(left), Makerbot used to fabricate the solid leg design(right)

the performance of both leg designs.

4.2.1 Experimental Setup

We built a rig using aluminium T-Slot bars to house the robot, and simulate obstacles at varying heights and distances.

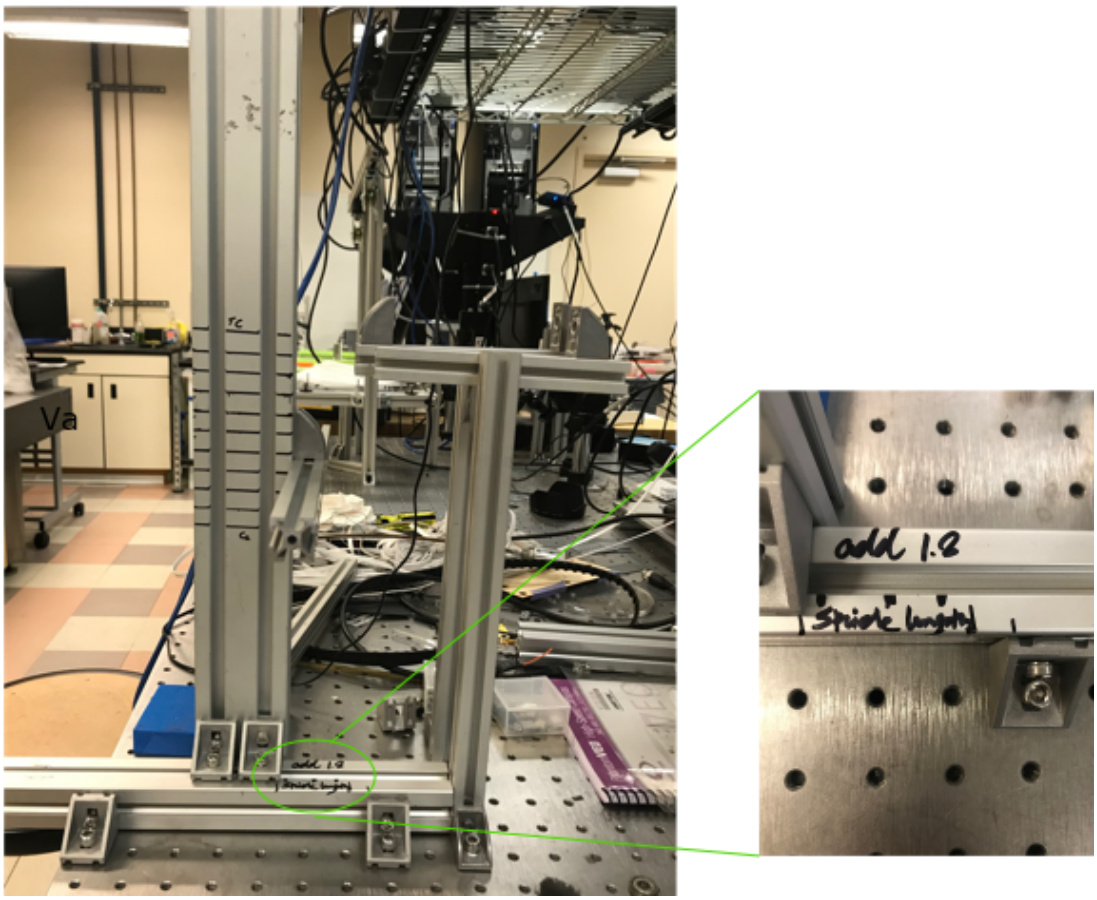

Figure 4.5: Compliant Leg Testing Rig. The markings of the right are the varying heights at which the obstacles were simulated and on the right the stride length along with the different lengths at which the tests were performed.

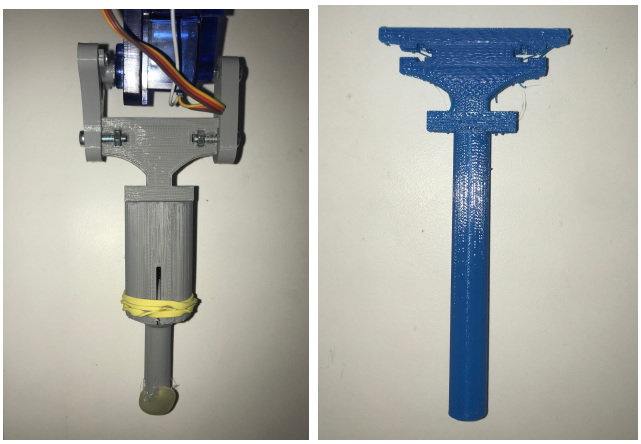

Figure 4.6: New compliant leg(right), New solid leg (left)

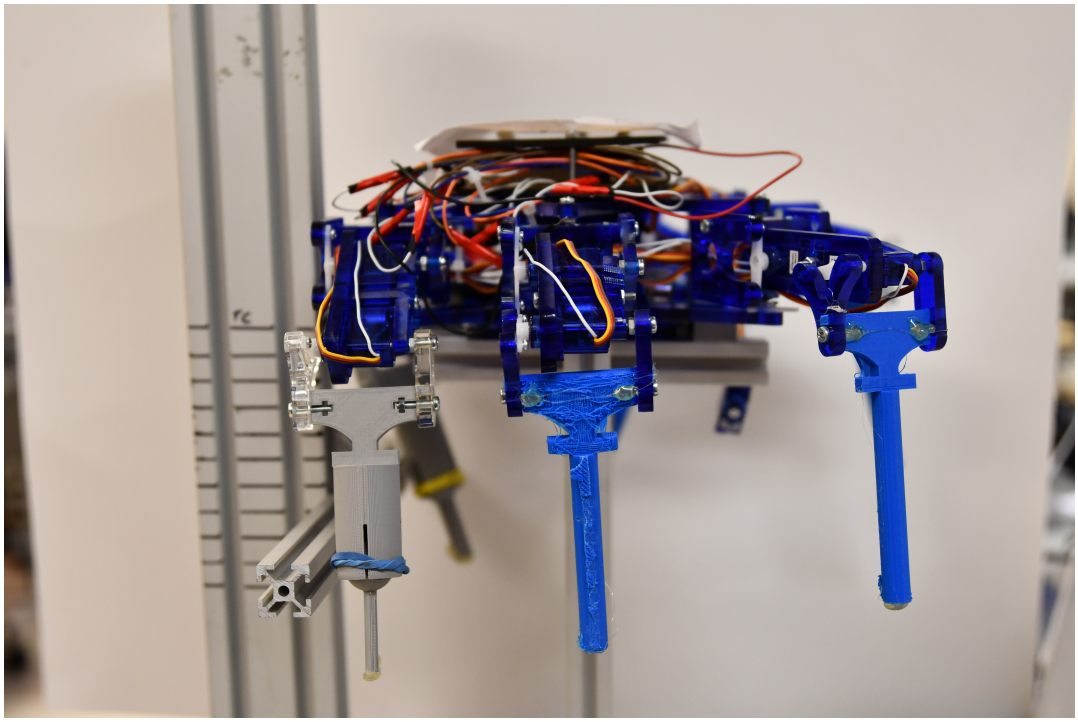

Figure 4.7: Side view of the robot housed on the rig

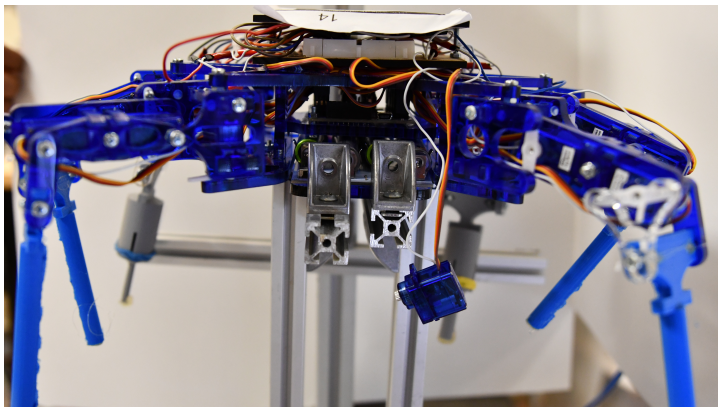

Figure 4.8: rear view of the robot housed on the testing rig

The height ranged from 0mm to the total ground clearance of the robot based on the new design. The other parameter was the distance of the obstacle from the robot. In the swing phase the leg, it retracts the foot and the thigh, while sweeping forward at the hip. This leads to a flattened sinusoidal phase of the leg and not a square wave. Due to this feature the height of the foot is constantly varying from the ground based on the angle swept by the hip. To study the possible effect of this feature we performed the experiments at three different distances from the starting position of the foot. As the stride length of the robot was 44mm, we chose the 3 different distances as 10mm, 20mm and 30mm representing the beginning middle and end of swing phase.

4.2.2 Designs performance comparisons

The plot below is a comparison of the performance of the two foot designs when encountering obstacles at different heights and distances. The axes of the plot are distance from the starting position of the leg and the height of the obstacle from the ground. This was done to understand the possible improvement in the robot's overall performance when traversing a rough terrain by replacing a solid leg with a compliant leg. In Figure 4.9 we can see that the compliant leg was able to cross higher obstacles.

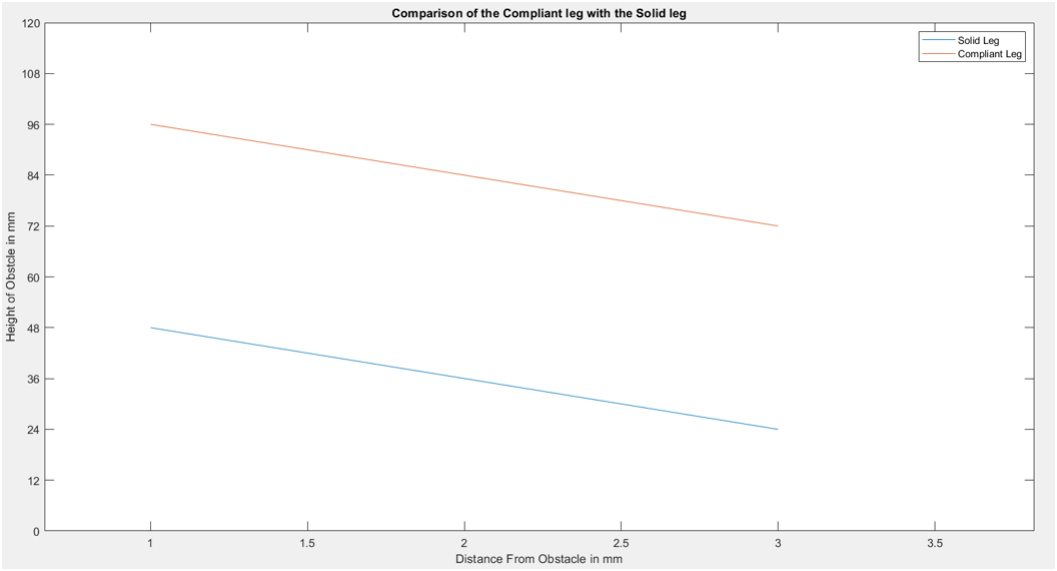

Figure 4.9: Comparison of the performance of the compliant leg vs the solid leg

4.2.3 Shear force Testing

The static testing of the robot using a simulated obstacle showed a huge advantage over the solid leg design in terms of performance over rough substrates. The next logical step was to make sure the new design was practical enough to be implemented onto the robot. The previous experiment tested the performance of the leg in the swing phase where the force acting on the leg was the impact force generated by the obstacle on collision. The force generated on collision was directly dependent on the torque of the hip Joint. As the hip provided the sweeping motion in a plane parallel to the ground to propagate the robot forward. Now, in the stance phase the force acting on the leg is a shear force also called the frictional force. Now,

$$F_K = N * \mu \tag{4.1}$$

where, N = Normal force,

μ = the friction coefficient of the leg.

In the stance phase, ideally there are three legs in contact with the ground. Distributing the weight of the robot equally. The weight of the robot with all the

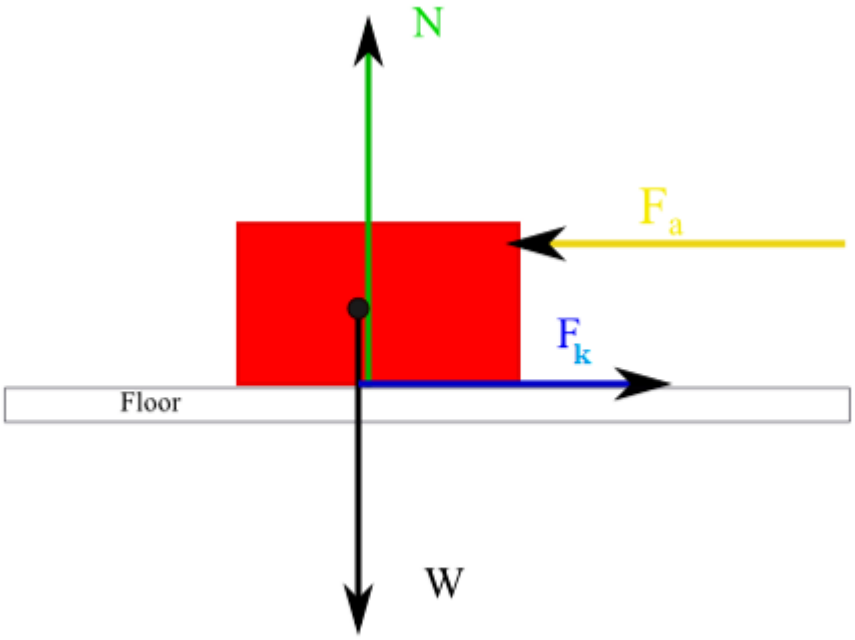

Figure 4.10: Basic concept of Friction Force

modifications is 1Kg.Therefore,

$$N = 333.33g, \tag{4.2}$$

$$\mu = 0.2[1] \tag{4.3}$$

$$F_K = N * \mu \tag{4.4}$$

$$F_K = 333.33 * 0.2 \tag{4.5}$$

$$F_K = 66.66g \tag{4.6}$$

Therefore, the new design should be able to sustain a shear force of at least $70g$ before deflection, this value was chosen by considering a slight tolerance. We performed the shear test on the new design both under compression and without. Under compression the leg performed as desired where the leg deflected by 3Degrees which was a feature of the design.Even when uncompressed the leg was able to bear a load of 70g with a minimal deflection of 5Deg. This meant that the spring could maintain the structure of the leg for locomotion in the uncompressed state too. We

then tested what the minimum necessary load was to reach maximum deflection in the leg.

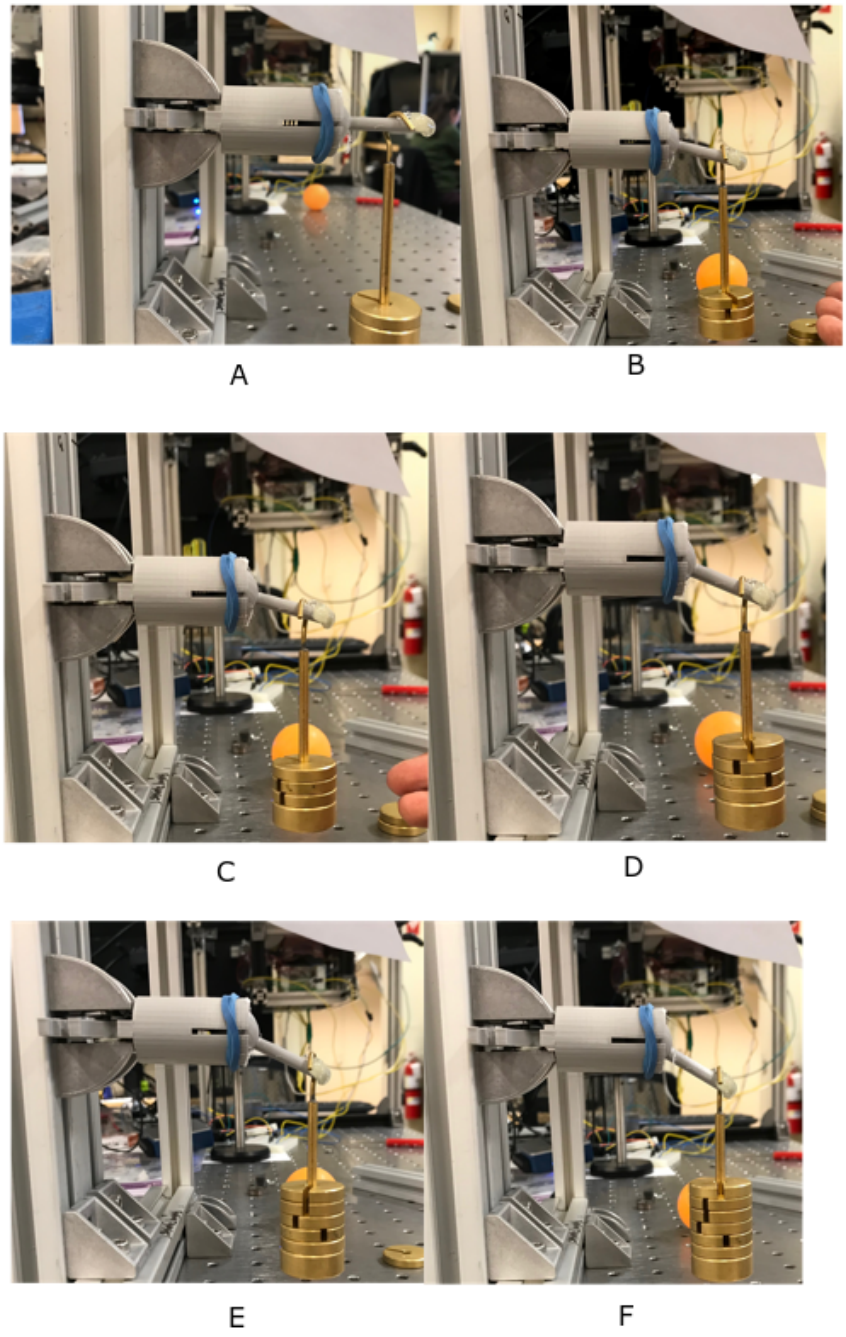

Figure 4.11: The pictures above are of the tests performed on the uncompressed compliant leg.(A) 70g, (B)90g, (C)110g, (D) 130g, (E) 150g, (F)170g

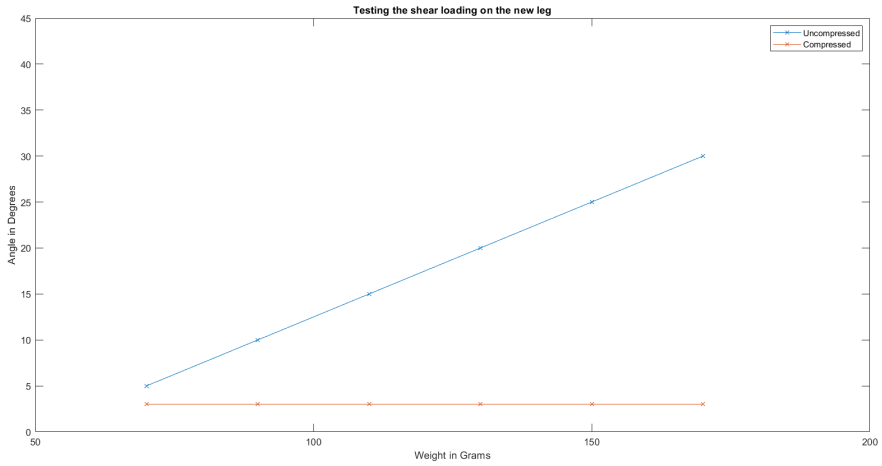

Figure 4.12: The reaction of the leg when shear force is applied both in the compressed and uncompressed conditions

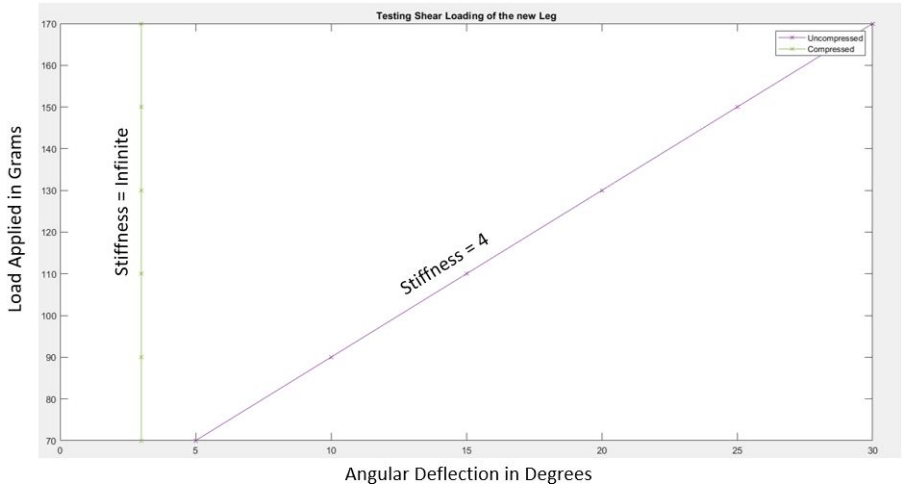

Figure 4.13: Stiffness comparison of the leg when compressed and uncompressed

The above results are mathematically supported too. The torque of the servo used is 2.5 kg-cm. Which is significantly more than the normal force acting on each leg during the stance phase. The slope of the above plot represents the inverse of mending stiffness. The leg when compressed has a slope of Zero, which translates to a Stiffness of Infinity signifing that the leg does not deform under the load applied. The leg when uncompressed has a stiffness of 4 .See table of servo Specs 2.1

4.3 Summary of Analysis

Based on the results from our experiments on the substrates with the whole robot. Two main points were in need to be answered. The possibility to traverse an obstacle higher than what a solid leg with similar dimensions can, and analyse the effect of the distance of the obstacle from the legs' initial position. The testing rig was designed to hold the robot in place while testing the different legs. In our tests the omnidirectional leg design was not truly put to the test. As in the highly controlled environment the obstacle was always directly in front of the leg. Also the use of a T-bar prevent the existence of a corner. From the results of testing we can observe that the compliant leg performs better than the solid leg when encountering taller obstacles. But, at the same time we also reinforced the idea of the correlation between the distance of the obstacle from the leg, i.e the relation of the size of an obstacle to the stride length. We can see that the robot can cross higher obstacles when they are in the first half of the swing Phase in comparison to the presence of an obstacle in the second half of the swing phase.

The next logical test would be to do full length runs with the robot. For the test to be effective the leg should be able to bear the weight of the robot and propel it forward. Therefore, we needed to test the performance of the leg design in the stance phase. Where, the force that can compromise the performance of the leg is the shear force due to friction. The leg under compression was able to sustain loads double the shear force generated by the normal reaction by maintaining integrity of the design. The leg when not compressed does not have the rigid material to prevent leg from deforming. Hence, the test was a direct correlation to the stiffness of the linear spring. As the leg even in the uncompressed state was able to sustain the load of the leg showed positive signs of success when implemented on the robot. While testing we found out that the leg would reach full deflection when loaded with 170g shear force. This was significantly less than the torque provided by the metal geared servos used in the robot, which was 2.5kg-cm.

Chapter 5

Conclusion and Future Work

5.1 Conclusion

The circular sprawled stance design of the robot is a very stable design and has a large range of operational speeds maintaining high stability. This design was chosen as we needed to establish the efficiency of the tripod gait over rough substrates. We used lab generated simulations of a rough surface, to control the no. of obstacles and their placement, and test the robot in a highly controlled environment. The block sizes of the checkerboard patterns were strategically chosen based on the stride length to assure contact. In our initial experiments the robot was made to traverse along the length of the substrate with varying success. During the experiments the angular position of the servos were recorded using a potentiometer. Simultaneously the position of the entire robot was also being monitored to get a higher level understanding of the effect of each interaction on the robot. These revealed many intricacies of the interactions taking place during each run. Based on the results of the different experiments we decided to implement a distributed mechanics system with compliant legs. To diffuse the disturbance created before it reached the hip joint and effected the stability of the entire robot. We designed a new compliant leg with omnidirectional compliance. To tackle obstacles from multiple directions. We then needed to test the performance of the new leg on interacting with obstacles and compare it to the solid leg design. Therefore, we decided to draw our focus onto the interactions of the legs with the obstacles.

We built a testing rig with a simulated obstacle at varying heights and distances to compare the success of the two designs. The compliant leg performed better than the solid leg by successfully crossing higher obstacles. The next step of the designing phase was to make sure the leg could sustain the robot in locomotion on a flat surface without deforming. To simulate the environment we tested the limits of the shear force acting on the tip of the foot. The results proved that the leg should be able to bear the weight of the robot an sustain locomotion on a flat surface.

5.2 Future Work

We would like to implement the legs on a robot and test the performance in terms of speed and stability of the robot.To establish a larger data set supporting our idea of the correlation between the stride length and the obstacle size. Implement the new leg at different positions on the robot to study the variation in the performance. utilize different kinematics where the robot is not limited by the practical clearance and can explore areas where the entire design clearance is needed. In the comparison of the performance of the robot across all the substrates ideally the flat runs should have a similar distribution as the runs in air. But in some instances there were some outliers. To understand the reason for this discrepancy we would like to add another layer of feedback in the form of force sensors at the tip of each foot. Ultimately, to bring the robot closer to the source of inspiration design a leg with higher degrees of freedom.

Bibliography

[1] Material Contact Properties Table. page 2, 2008.

[2] P. Birkmeyer, K. Peterson, and R. S. Fearing. DASH: A dynamic 16g hexapedal robot. *2009 IEEE/RSJ International Conference on Intelligent Robots and Systems, IROS 2009*, pages 2683–2689, 2009.

[3] James D. Crall, Nick Gravish, Andrew M. Mountcastle, and Stacey A. Combes. BEEtag: A low-cost, image-based tracking system for the study of animal behavior and locomotion. *PLoS ONE*, 10(9):1–13, 2015.

[4] Hua Deng, Guiyang Xin, Guoliang Zhong, and Michael Mistry. Gait and trajectory rolling planning and control of hexapod robots for disaster rescue applications. *Robotics and Autonomous Systems*, 95:13–24, 2017.

[5] Ioan Doroftei and Florentina Adascalitei. A hexapod walking micro-robot with compliant legs. *Applied Mechanics and Materials*, 162(October):234–241, 2012.

[6] Xingji Duan, Weihai Chen, Shouqian Yu, and Jingmeng Liu. Tripod gaits planning and kinematics analysis of a hexapod robot. *2009 IEEE International Conference on Control and Automation, ICCA 2009*, pages 1850–1855, 2009.

[7] Daniel M. Dudek and Robert J. Full. An isolated insect leg's passive recovery from dorso-ventral perturbations. *Journal of Experimental Biology*, 210(18):3209–3217, 9 2007.

[8] Thomas Endlein and Walter Federle. On heels and toes: How ants climb with adhesive pads and tarsal friction hair arrays. *PLoS ONE*, 10(11):1–16, 2015.

[9] Kenneth S. Espenschied, Roger D. Quinn, Randall D. Beer, and Hillel J. Chiel. Biologically based distributed control and local reflexes improve rough terrain locomotion in a hexapod robot. *Robotics and Autonomous Systems*, 18(1-2):59–64, 1996.

[10] R. J. Full, R. Blickhan, and L. H. Ting. Leg design in hexapedal runners. *The Journal of experimental biology*, 158:369–390, 1991.

[11] R. J. Full and M. S. Tu. Mechanics of a rapid running insect: Two-, four- and six-legged locomotion. *Journal of Experimental Biology*, 156:215–231, 1991.

[12] Martyna Grabowska, Elzbieta Godlewska, Joachim Schmidt, and Silvia Daun-Gruhn. Research article: Quadrupedal gaits in hexapod animals - inter-leg coordination in free-walking adult stick insects. *Journal of Experimental Biology*, 215(24):4255–4266, 2012.

[13] Dariusz Grzelczyk, Bartosz Stanczyk, and Jan Awrejcewicz. Kinematics, Dynamics and Power Consumption Analysis of the Hexapod Robot during Walking with Tripod Gait. *International Journal of Structural Stability and Dynamics*, 17(5), 2017.

[14] Aaron M. Hoover, Samuel Burden, Xiao Yu Fu, S. Shankar Sastry, and R. S. Fearing. Bio-inspired design and dynamic maneuverability of a minimally actuated six-legged robot. *2010 3rd IEEE RAS and EMBS International Conference on Biomedical Robotics and Biomechatronics, BioRob 2010*, pages 869–876, 2010.

[15] Ke Jung Huang, Chun Kai Huang, and Pei Chun Lin. A simple running model with rolling contact and its role as a template for dynamic locomotion on a hexapod robot. *Bioinspiration and Biomimetics*, 9(4), 2014.

[16] Gao Jianhua. Design and kinematic simulation for Six-DOF Leg Mechanism of hexapod robot. *2006 IEEE International Conference on Robotics and Biomimetics, ROBIO 2006*, (50405012):625–629, 2006.

[17] Sangbae Kim, Jonathan E. Clark, and Mark R. Cutkosky. ISprawl: Design and tuning for high-speed autonomous open-loop running. *International Journal of Robotics Research*, 25(9):903–912, 2006.

[18] Bernhard Klaassen, Ralf Linnemann, Dirk Spenneberg, and Frank Kirchner. Biomimetic walking robot SCORPION: Control and modeling. *Robotics and Autonomous Systems*, 41(2-3):69–76, 2002.

[19] R. Kram, B. Wong, and R. J. Full. Three-dimensional kinematics and limb kinetic energy of running cockroaches. *Journal of Experimental Biology*, 200(13):1919–1929, 1997.

[20] Serdar Küçük. *Serial and Parallel Robot Manipulators*. 2012.

[21] Roger D. Quinn, Gabriel M. Nelson, Richard J. Bachmann, Daniel A. Kingsley, John T. Offi, Thomas J. Allen, and Roy E. Ritzmann. Parallel complementary strategies for implementing biological principles into mobile robots. *International Journal of Robotics Research*, 22(3-4):169–186, 2003.

[22] Lars Reinhardt, Tom Weihmann, and Reinhard Blickhan. Dynamics and kinematics of ant locomotion: Do wood ants climb on level surfaces? *Journal of Experimental Biology*, 212(15):2426–2435, 2009.

[23] Xochitl Yamile Sandoval-Castro, Mario Garcia-Murillo, Luis Alberto Perez-Resendiz, and Eduardo Castillo-Castañeda. Kinematics of Hex-piderix - A six-legged robot - Using screw theory. *International Journal of Advanced Robotic Systems*, 10, 2013.

[24] Uluc Saranli, Martin Buehler, and Daniel E. Koditschek. RHex: A simple and highly mobile hexapod robot. *International Journal of Robotics Research*, 20(7):616–631, 2001.

[25] Robert T. Schroer, Matthew J. Boggess, Richard J. Bachman, Roger D. Quinn, and Roy E. Ritzmann. Comparing cockroach and whegs robot body motions. *Proceedings - IEEE International Conference on Robotics and Automation*, 2004(4):3288–3293, 2004.

[26] Franco Tedeschi and Giuseppe Carbone. Design issues for hexapod walking robotsdesign issues for hexapod walking robots. *Robotics*, 3(2):181–206, 2014.

[27] L. H. Ting, R. Blickhan, and R. J. Full. Dynamic and static stability in hexapedal runners. *The Journal of experimental biology*, 197:251–269, 1994.

[28] J. T. Watson and R. E. Ritzmann. Leg kinematics and muscle activity during treadmill running in the cockroach, Blaberus discoidalis: I. Slow running. *Journal of Comparative Physiology - A Sensory, Neural, and Behavioral Physiology*, 182(1):11–22, 1997.

[29] G M Werner and M G Dyer. Evolution of communication in artificial organisms. *Artificial life II*, (June 2014):659–687, 1991.

[30] David Zarrouk and Ronald S. Fearing. Compliance-based dynamic steering for hexapods. *IEEE International Conference on Intelligent Robots and Systems*, pages 3093–3098, 2012.

[31] Guoliang Zhong, Long Chen, Zhongdong Jiao, Junfeng Li, and Hua Deng. Locomotion Control and Gait Planning of a Novel Hexapod Robot Using Biomimetic Neurons. *IEEE Transactions on Control Systems Technology*, 26(2):624–636, 2018.

[32] Christoph P E Zollikofer. Stepping Patterns in Ants. *Journal of Experimental Biology*, 192:119–127, 1994.